ABSTRACT

JAMES, CHRIS MARY. Adaptive Transmission Using Channel Inversion for Multiple-Antenna Systems. (Under the direction of Professor Brian L. Hughes.)

Adaptive modulation often achieves a significantly higher capacity than nonadaptive modulation in multiple-antenna wireless communication systems, particularly when the transmit antennas outnumber the receive antennas. Adaptive modulation generally involves varying signal power, constellation and coding in response to changing channel conditions, which adds considerable system complexity. This thesis examines simpler adaptive transmission schemes based on channel inversion (CI) and truncated channel inversion (TCI) in combination with multi-dimensional eigen-beamforming. Optimal CI and TCI schemes for multiple-antenna systems are derived and it is shown that these schemes suffer a small loss in capacity relative to optimal adaptive modulation, even for relatively small antenna arrays. This thesis also considers a practical coding scheme, turbo trellis-coded modulation (TTCM) in conjunction with CI. The results indicate that this scheme can perform within 4 dB of the optimal adaptive capacity.

Adaptive Transmission Using Channel Inversion for Multiple-Antenna Systems

by

Chris Mary James

A thesis submitted to the Graduate Faculty of
North Carolina State University
in partial fulfillment of the
requirements for the Degree of
Master of Science

Department of Electrical and Computer Engineering

Raleigh

December 22, 2004

Approved By:

Dr. J. Keith Townsend

Dr. Rudra Dutta

Dr. Brian L. Hughes
Chair of Advisory Committee

To my husband, my parents and my sister . . .

Biography

Chris Mary James was born in Trivandrum, India on December 4, 1977. She received her B.E.(Hons) degree in Electrical and Electronics Engineering from Birla Institute of Technology and Science, Pilani, India. She worked for nearly 11 months for the Global Services Division of Wipro in Bangalore, India. She is now currently working towards the completion of her Master of Science degree in Electrical Engineering at North Carolina State University.

Acknowledgements

I would like to extend my heartfelt thanks to my advisor, Dr. Brian Hughes for his guidance in my research and for his understanding and support during the difficult times I have had during the duration of my program. I would like to express my gratitude to Dr. Keith Townsend and Dr. Rudra Dutta for being on my thesis committee and providing me valuable feedback on various aspects of my thesis. I would also like to thank Dr. Alexandra Duel-Hallen for her input during my qualifying review. My thanks to Xinying Yu, my colleague, who has been an inspiration to me with her hard work, and also to all my colleagues in the lab, Ajith Kamath, Pallav Sudarshan, Sandeep Krishnamoorthy and Mahmud Jalnase for their help with research and for their friendship. They made my time spent at North Carolina State University really enjoyable. Last but not the least, I would like to say thank you to my husband, Piyush Shivam, for all the technical and moral support he has given me the last two and a half years. If not for him, I would not have reached this far today.

Contents

List of Tables

List of Figures

Chapter 1

Introduction

The goal of future wireless systems is to allow seamless access to information virtually anywhere at anytime. The technology trend is also toward higher and higher data rates with continued demand for higher quality of services. Fourth generation systems are envisioned to support high mobility and bit rates greater than 10 Mbps [1].

Designing very high-speed wireless links that can transmit voice, images and other types of multimedia date reliably constitutes a significant research and engineering challenge. The available radio spectrum is scarce and must be allocated to many different applications and systems. Spectral efficiency, defined as the average data rate per unit bandwidth for a specified transmit power and bit-error-rate (BER), is therefore of primary concern in the design of future wireless communications systems.

Unfortunately transmission over wireless links is characterized by time-varying multipath fading in which a transmitted signal arrives at the receiver through multiple reflective paths with random delays [2]. This can cause fluctuations in the received signal-to-noise ratio (SNR) resulting in a high BER. Fading compensations techniques like interleaving with channel coding and fixed link margin can be employed to maintain acceptable performance during deep fades. However these non-adaptive techniques are often designed for worst-case channel conditions and this leads to unnecessary wastage of the channel capacity.

Since the demand for high data rate wireless applications is growing at an explosive pace, it is essential to exploit the full capacity potential of the wireless fading channel. One of the ways to achieve this goal is to employ adaptive transmission techniques. Adapting parameters of the transmitted signal to the changing fade values when the channel state information (CSI) is available at the transmitter allows the channel to be utilized more efficiently [3].

Adaptive modulation was first proposed in the late 1960s [4] but recently considerable research effort has focused on adaptive transmission as a means to improve spectral efficiency on time-varying fading channels. The transmitted power level [4, 5], symbol transmission rate [6], constellation size [7, 8, 9, 10], coding rate/scheme [11, 12, 13] or any combination of these parameters [14, 15, 16, 17, 18] can be adapted based on the instantaneous fade value. All these schemes seek to increase the data rate, without sacrificing BER by transmitting at high speeds under favorable channel conditions and reducing throughput as the channel degrades.

Critical to adaptive modulation is the quality of CSI at the transmitter and this can be estimated at the receiver and sent to the transmitter via a feedback channel. The availability of perfect channel knowledge at the transmitter is practical only as long as the channel fading is slow relative to the data rate. Delays and errors introduced by feedback and/or estimation can lead to serious degradation in the performance of adaptive techniques designed assuming perfect CSI [14]. Using long-range channel prediction methods [19, 20] and/or accounting for CSI imperfections explicitly when designing adaptive techniques [21] help in ensuring robust schemes.

Information theoretic results indicate that multiple-antenna systems can further enhance performance and capacity when perfect or partial CSI is made available at the transmitter [22, 23, 24]. By utilizing space as an additional dimension, these multiple-antenna systems employing adaptive techniques surpass the data rates achieved by conventional systems utilizing time and frequency alone [25, 26, 27, 28, 29]. When the channel varies rapidly it is not always meaningful to acquire instantaneous CSI because it becomes outdated. For such scenarios, [30, 31, 32, 33, 34, 35] have derived transmission schemes for multiple-antenna systems based on the statistics of the underlying channel.

Throughout the thesis, we assume the availability of perfect channel state information at both the transmitter and the receiver, and as we saw before, this assumption is reasonable provided the channel is slowly varying. It is well known that in such a scenario where the transmitter has perfect CSI, the capacity of a multiple-input multiple-output (MIMO) system is achieved by decomposing the system into parallel subchannels through a singular value decomposition (multi-dimensional eigen-beamforming) with the transmitter sending independent data streams across these subchannels. The optimal power adaptation is shown to be water-filling over space and time [36]. In general, this optimal adaptive capacity can be approached by varying signal power, constellation, and coding in response to changing channel conditions and this adds considerably to the system complexity. Consequently, it is natural to investigate the use of simpler adaptive techniques, particularly those that leverage the extensive literature on codes designed for additive white Gaussian noise (AWGN) channels.

One of the simplest adaptive transmission techniques is channel inversion (CI) [3, 14], in which the transmitter seeks to maintain a constant SNR at the receiver, thereby effectively converting it to an AWGN channel. Channel inversion is not suitable for single-antenna systems experiencing Rayleigh fading [3], since an infinite average transmitted power is required to maintain any positive SNR at the receiver. However, when CI is combined with receive diversity, the capacity penalty decreases quickly with the number of diversity branches [29].

In this thesis we investigate adaptive transmission schemes that combine channel inversion with multi-dimensional eigen-beamforming. During the course of our work, we became aware of similar research that sought to apply channel inversion to multiple-antenna systems [37, 38, 39]. But unlike these papers, we do not constrain the SNRs in each subchannel of our decomposed MIMO system to be equal, but instead for a fixed average transmitter power, we derive optimal SNR targets that maximize the overall capacity of the channel. The removal of the equal SNR constraint enables our scheme to exhibit superior performance. The SNR targets are shown to obey a kind of "weighted" waterfilling distribution.

We also consider the use of truncated channel inversion (TCI) [3] for multiple-antenna systems and the capacity gain relative to CI is shown to be minimal for most cases. Outage capacities for each of the adaptive transmission schemes are also explored. For all but the smallest MIMO systems, our results suggest that most of the adaptive capacity of MIMO channels can be achieved by systems that combine eigen-beamformer channel inversion with fixed constellations and error-control codes designed for the AWGN channel.

In 1993, powerful turbo codes [40] were introduced for binary modulation which achieve good bit-error-rates at low SNRs for AWGN channels. Recent efforts [41, 42, 43, 44, 45] have looked at combining binary turbo codes with higher order modulation. This thesis focuses on applying one of those high spectral efficiency turbo codes — turbo trellis-coded modulation (TTCM) introduced by Robertson *et al* [43] to the channel inversion scheme for multiple-antenna systems.

In TTCM, the basic principle of binary turbo codes is applied to Ungerboeck's trellis-coded modulation [46] so that the important properties and advantages of both the codes can be retained. TTCM is not the best code known today for AWGN channels, but due to its simplicity, it is implemented and the spectral efficiency compared with the theoretical maximum. Using some of the other coding schemes and/or better encoders and better interleaver design, it is possible to improve and achieve spectral efficiency within a fraction of the channel inversion capacity for multiple-antenna systems.

The rest of this thesis is organized as follows. In Chapter 2, we describe characteristics of wireless fading channels with particular emphasis on Rayleigh fading channels. The channel model is introduced and capacities for optimal adaptive and nonadaptive transmission are reviewed. We also motivate the need for a simple adaptive transmission technique which simplifies receiver and transmitter design while suffering minimal capacity loss from optimal.

In Chapter 3, we propose the new simple suboptimal transmission scheme in which channel inversion and truncated channel inversion is applied with multi-dimensional eigen-beamforming to MIMO systems. Ergodic and outage capacities for the schemes are explored and compared with other schemes. Since the new schemes allow us to use fixed rate modulations, we also derive constellation-constrained capacities.

In Chapter 4, we apply turbo trellis-coded modulation, which has shown reasonably good results in AWGN channels to our channel inversion scheme. We find that this practical scheme gets us to within 4 dB of the optimal adaptive capacity.

Finally, in Chapter 5, we summarize our conclusions and offer some possible research directions for the future.

Chapter 2

Overview

In this chapter, we briefly review the characteristics of fading channels with emphasis on Rayleigh fading. We also introduce the channel model that is used throughout the thesis and review the optimal adaptive and nonadaptive transmission schemes.

The notation we follow throughout the rest of the thesis is presented here: Bold uppercase (lowercase) letters denote matrices (column vectors); $(\cdot)^\dagger$ denotes Hermitian transpose; $\mathcal{E}\left[\cdot\right]$ stands for expectation, $\mathbf{I}_K$ denotes the identity matrix of size K. The special notation $\mathbf{n} \sim \mathcal{CN}(\bar{n}, \mathbf{\Sigma}_n)$ indicates that $\mathbf{n}$ is complex Gaussian distributed with mean $\bar{n}$ and covariance matrix $\mathbf{\Sigma}_n$.

2.1 Fading

Fading is the rapid fluctuation of the amplitude of a radio signal over a short period of time or travel distance [47]. In a mobile radio environment, the transmitted signal often propagates to the receiver via multiple paths due to reflection, diffraction and/or scattering as illustrated in Fig. 2.1. These multiple signals from different propagation paths arrive with different delays and combine vectorially at the receiver to give a resultant signal which varies widely in amplitude and phase.

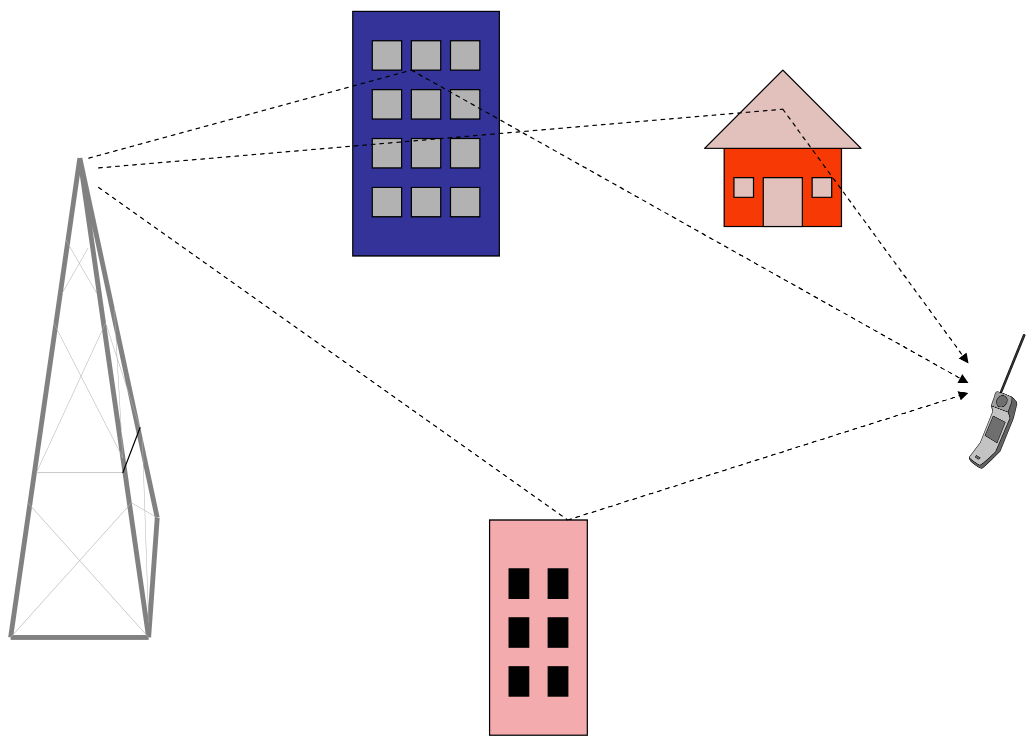

Figure 2.1: Multipath fading

The relation between the signal parameters such as bandwidth, symbol period etc.

and the channel parameters such as Doppler spread will determine the types of fading experienced by different transmitted signals [47]. In narrowband systems, the multipath components of the transmitted signal often arrive at the receiver within a small fraction of the symbol duration, resulting in what is known as frequency-nonselective or flat fading. When a signal experiences flat fading, the spectral characteristics of the transmitted signal are unchanged at the receiver. However the amplitude of the received signal changes with time due to fluctuations in the gain of the channel caused by multipath. If the line-of-sight component is absent, the signal received at the output of a flat-fading wireless channel is usually modeled as having a Rayleigh distributed amplitude and a uniformly distributed phase. The Rayleigh distribution has a probability density function (pdf) given by

$$p(a) = \begin{cases} \frac{a}{\sigma^2} e^{(-a^2/2\sigma^2)} & a \geq 0; \\ 0 & a < 0. \end{cases} \tag{2.1}$$

where a is the envelope amplitude of the received signal and $2\sigma^2$ is the pre-detection mean power of the multipath signal.

However, in wideband systems, the time spread of the multipath components is often large compared to the reciprocal bandwidth of the transmitted message form and this leads to frequency-selective fading. In this situation the channel introduces amplitude and phase distortion to the message waveform and the spectrum of the channel varies over the signaling bandwidth. This leads to intersymbol interference between transmitted symbols.

In many situations, the transmitter, the receiver and/or several of the scatterers can be in motion. In such a case, the experienced frequency of a transmitted signal at the receiver will be slightly different from the actual transmitted frequency and this shift in frequency is referred to as Doppler shift. Relative motion in the wireless environment can cause different Doppler shifts among the multipath signal components resulting in time-variant signal fading. When the Doppler bandwidth is small compared with the inverse bandwidth of the signal, the fading is considered slow and the attenuation is approximately constant for several symbols. Otherwise, the fading is considered fast.

2.2 Channel Model

Consider the single user baseband channel model illustrated in Fig. 2.2 in which t transmit antennas are used to send data to r receive antennas. The discrete-time baseband equivalent channel model is given by

$$\mathbf{y} = \mathbf{H}\mathbf{x} + \mathbf{n} \tag{2.2}$$

where $\mathbf{H}$ is a $r \times t$ complex channel matrix, with the (i, j) th element representing the fading between the i-th receive and j-th transmit antenna. Here, $\mathbf{x}$ is a $t \times 1$ vector of complex transmitted signals with x_i being the symbol transmitted from the i-th transmit antenna and $\mathbf{y}$ is an $r \times 1$ vector of received signals with y_j being the signal detected at the the j-th receive antenna. We assume that $\mathbf{n}$ is an additive noise source and is modeled as a zero mean circularly symmetric complex Gaussian random vector with statistically independent elements, that is, $\mathbf{n} \sim \mathcal{CN}(\mathbf{0}, \mathbf{I}_r)$. The total average transmit power or the average power at each receive antenna is constrained to be at most P irrespective of the number of transmit antennas: $\mathcal{E}[\mathbf{x}^\dagger \mathbf{x}] = \mathrm{tr}\left(\mathcal{E}[\mathbf{x}\mathbf{x}^\dagger]\right) \leq P$.

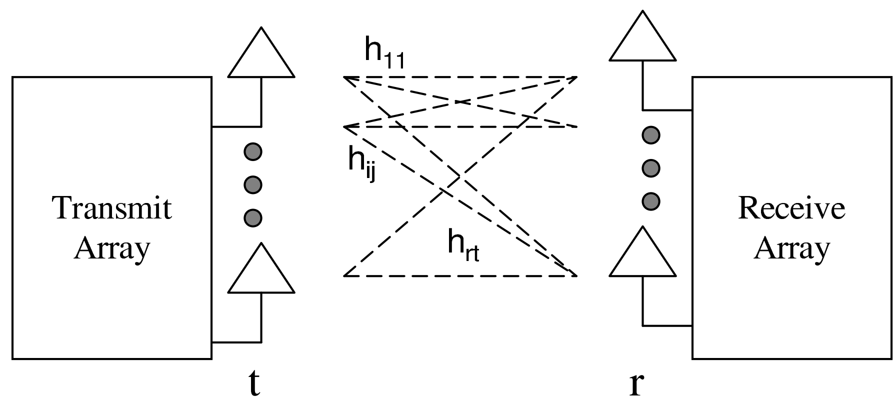

Figure 2.2: Channel model

It is assumed that each use of the channel corresponds to an independent realization of $\mathbf{H}$. The entries of $\mathbf{H}$ are restricted to be independent and identically distributed (i.i.d.) Gaussian collection with independent real and imaginary parts, each with mean 0 and variance 1/2. Equivalently each entry of $\mathbf{H}$ has uniform phase and Rayleigh magnitude. This choice models a Rayleigh fading environment. The antennas are spaced far enough apart at both the transmitter and the receiver to ensure independent fading for each transmitting and receiving antenna pair [24].

By the singular value decomposition (SVD), $\mathbf{H}$ can be written as $\mathbf{H} = \mathbf{U}\mathbf{D}\mathbf{V}^\dagger$, where $\mathbf{U}$ and $\mathbf{V}$ are unitary matrices and $\mathbf{D}$ is a $r \times t$ diagonal matrix. In fact the diagonal entries of $\mathbf{D}$ are the non-negative square roots of the eigenvalues of $\mathbf{H}\mathbf{H}^\dagger$. Substituting the SVD for $\mathbf{H}$, (2.2) can be written as

$$\mathbf{y} = \mathbf{U}\mathbf{D}\mathbf{V}^\dagger\mathbf{x} + \mathbf{n}\ . \tag{2.3}$$

Multiplying $\mathbf{U}^\dagger$ on both sides, (2.3) can be rewritten as

$$\tilde{\mathbf{y}} = \mathbf{D}\tilde{\mathbf{x}} + \tilde{\mathbf{n}} \tag{2.4}$$

where $\tilde{\mathbf{x}} = \mathbf{V}^\dagger\mathbf{x}$, $\tilde{\mathbf{y}} = \mathbf{U}^\dagger\mathbf{y}$ and $\tilde{\mathbf{n}} = \mathbf{U}^\dagger\mathbf{n}$. Noticing that the distribution of $\tilde{\mathbf{n}}$ is invariant under unitary transformation, the multiple-antenna channel is equivalent to $\min(r,t)$ independent parallel Gaussian subchannels parameterized by the ordered gains $\lambda_1^{1/2}, \ldots, \lambda_m^{1/2}$ where $\lambda_1^{1/2} \geq \lambda_2^{1/2} \geq \ldots \geq \lambda_m^{1/2}$. The λ_is are the singular values of the fading matrix $\mathbf{H}$.

The above equation can be written component-wise as

$$\tilde{y}_i = \lambda_i^{1/2}\tilde{x}_i + \tilde{n}_i, \quad 1 \leq i \leq m = \min(r,t)\ . \tag{2.5}$$

2.3 Adaptive and Nonadaptive Transmission

Mutual information is a measure of the amount of information that one random variable contains about another random variable. For a channel $\mathbf{H}$ with input $\mathbf{x}$ and output $\mathbf{y}$, the mutual information in bits/sec/Hz is given by

$$I(\mathbf{x};\mathbf{y}) = \sum_{i=1}^{m} \log_2(1 + P_i\lambda_i) \tag{2.6}$$

where P_i is the power allocated to the i-th subchannel. The P_is are chosen to satisfy the power constraint P.

Capacity of the channel is defined as the maximum of the mutual information between the input and output over all distributions on the input that satisfy the power constraint [48], i.e., the capacity C is given by:

$$C = \max_{p(\mathbf{x}):tr\left(\mathcal{E}\left[\mathbf{x}\mathbf{x}^{\dagger}\right]\right)\leq P} I\left(\mathbf{x};\mathbf{y}\right) \tag{2.7}$$

where $p(\mathbf{x})$ is the probability distribution of $\mathbf{x}$ and $tr(\mathbf{A})$ is the trace of matrix $\mathbf{A}$. It is shown in [24] that the input distribution that maximizes this is circularly symmetric complex Gaussian.

When both the transmitter and the receiver know the fading matrix $\mathbf{H}$, the transmitter can adapt the rate of information transmission and power allocated across the subchannels according to the quality of the channel. The optimal power allocation strategy that maximizes (2.6) is given by:

$$P_i = \left(\frac{1}{\lambda_0} - \frac{1}{\lambda_i}\right)^{+} \tag{2.8}$$

where λ_0 is the cutoff value [24] and $(x)^{+} = \max(x, 0)$. If the fade value λ_i of the i-th subchannel is below the cutoff, then no data is transmitted on that subchannel. The cutoff value is found by solving

$$\sum_{i=1}^{m}\left(\frac{1}{\lambda_0} - \frac{1}{\lambda_i}\right)^{+} = P\ . \tag{2.9}$$

This power adaptation policy is called water-filling in space and the concept is illustrated in Fig. 2.3. The different bars represent the inverse of the the fade values of each subchannel. The power is poured over the subchannels to a constant level of $1/\lambda_0$. The power allocated to subchannel i equals $1/\lambda_0 - 1/\lambda_i$ provided $\lambda_i > \lambda_0$. The intuitive idea behind water-filling is to send more power in the subchannels which are good and less power on the degraded subchannels. If the instantaneous fade value of the subchannel is below the cutoff value, the channel is not used.

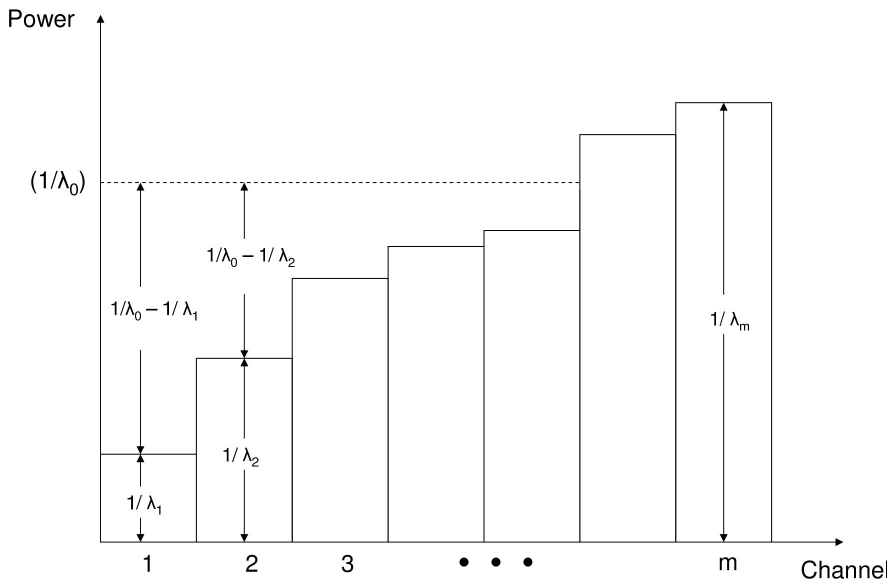

Figure 2.3: Water-filling in space

Therefore, the capacity or maximum mutual information of (2.6) with the optimal power adaptation reduces to

$$C = \sum_{i=1}^{m} \log_2 \left(\frac{\lambda_i}{\lambda_0} \right)^{+} . \tag{2.10}$$

The capacity in (2.10) is a random variable and fluctuates with channel matrix **H**. By averaging this over all the channel matrix realizations, we obtain Shannon or ergodic capacity. The Shannon capacity for single-antenna systems with channel side information at both transmitter and receiver was first derived by Goldsmith *et al* in [3]. It was shown that this capacity is achieved by a multiplexing technique whereby the signal transmitted over the channel is optimized for the instantaneous fade level. The resulting transmission scheme requires varying both the power and the rate.

In general, for a MIMO system with t transmit antennas and r receive antennas, when perfect CSI is available instantaneously at the transmitter, total power can be allocated adaptively not only over time but across the $m = \min(t, r)$ subchannels to achieve the highest possible bit rate. This is referred to as water-filling in space and time [36]. (When there is only one subchannel, the optimal power adaptation is referred to as water-filling in time [3].) The resulting optimal adaptation ergodic capacity of the MIMO channel is given by

$$C_{opt} = \sum_{i=1}^{m} \mathcal{E}\left[\log\left(1 + P_i \lambda_i\right)\right] \tag{2.11}$$

where $\mathcal{E}$ here denotes expectation with respect to the random gains $\lambda_1, \ldots, \lambda_m$ of the subchannels, and

$$P_i = \left(\frac{1}{\lambda_0} - \frac{1}{\lambda_i}\right)^+ \tag{2.12}$$

with λ_0, the cutoff value, chosen such that $\mathcal{E}\left[\sum_i P_i\right] = P$.

A suboptimal transmission scheme when $\mathbf{H}$ is known at the transmitter is to adapt the rate but maintain constant and equal power across the $m = \min(t, r)$ subchannels obtained by singular value decomposition. The capacity in this case, which we refer to as beamforming ergodic capacity is given by

$$C_{bm} = \sum_{i=1}^{m} \mathcal{E}\left[\log\left(1 + \frac{P}{m}\lambda_i\right)\right] \tag{2.13}$$

When the transmitter has no knowledge of the channel variation, it is optimal to distribute the power equally over the t transmit antennas [24]. The ergodic capacity for nonadaptive transmission is given by

$$C_{na} = \sum_{i=1}^{m} \mathcal{E}\left[\log\left(1 + \frac{P}{t}\lambda_i\right)\right] \tag{2.14}$$

In Fig. 2.4, we plot the ergodic capacity curves for optimal adaptation, beamforming and nonadaptive transmission for different $t \times r$ systems. It is interesting to note that the beamforming capacity and the nonadaptive capacity are the same in all cases except 4×2 since the number of transmit antennas equal the number of subchannels. Thus for i.i.d. fading, side information at the transmitter does not lead to any capacity benefit when the power is not adapted. However in realistic environments most channels exhibit correlated fading and in such cases, not adapting at the transmitter causes both a decrease in capacity and an increase in encoding and decoding complexity [3]. It is also seen that adaptive transmission outperforms nonadaptive transmission for all systems at low SNRs, but the performance difference is significant at high SNRs only when $t > r$. Beamforming strategy is suboptimal to optimal adaptation at low SNRs but at high SNRs the two power allocation strategies are close to each other.

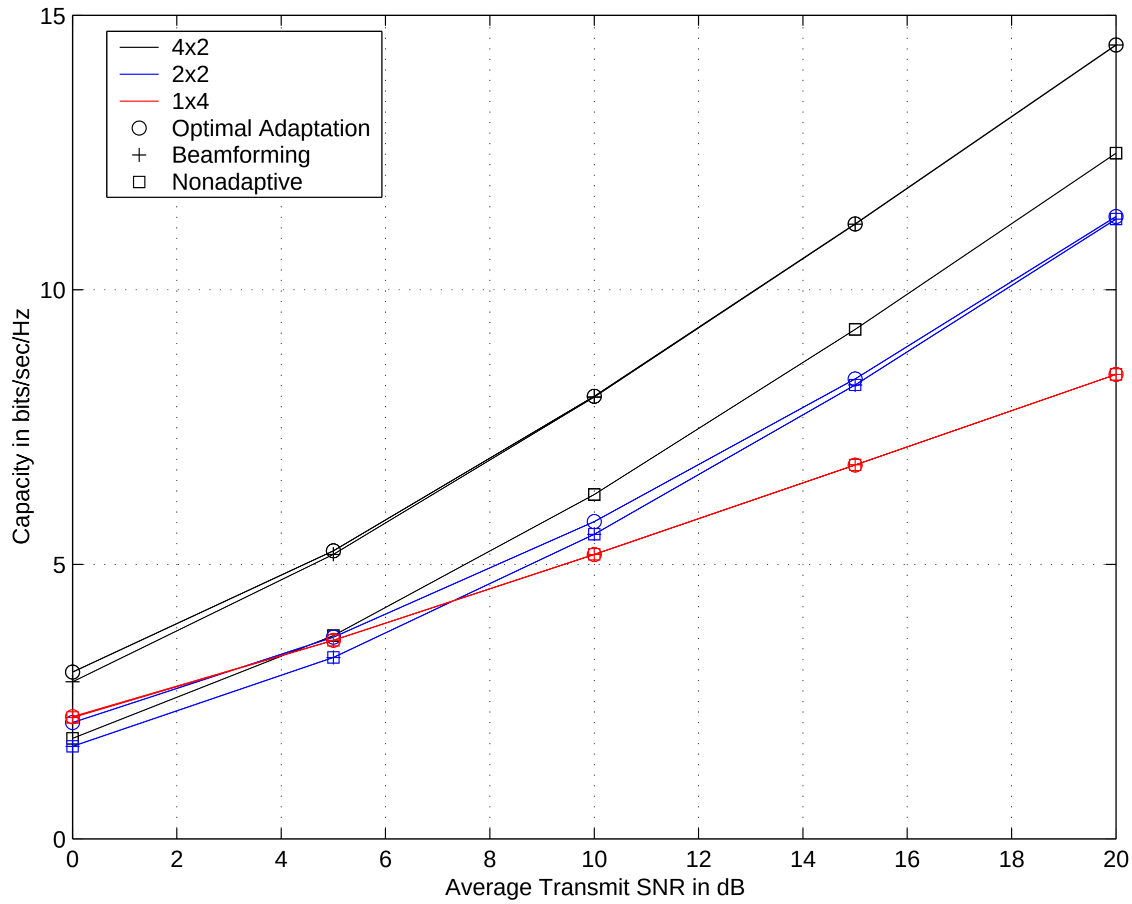

Figure 2.4: Capacities of different transmission schemes

2.4 Background

Optimal adaptive transmission outperforms nonadaptive transmission especially when $t > r$. In general, approaching the optimal adaptive capacity requires adapting the transmitter's power, constellation and error-control code to changing channel conditions. This adds considerably to the system complexity. Beamforming that performs close to optimal adaptive capacity especially at high SNRs simplifies transmitter design since power is not adapted. However the receiver design for the beamforming scheme is complicated since it sees varying instantaneous fade values. This drives the need for adaptive schemes that not only simplify transmitter design but also receiver design and in addition can leverage the extensive literature on codes designed for the AWGN channel.

Generally in the literature $\mathbf{H}$ is assumed to be known at the receiver. However throughout this thesis, for any adaptive scheme under consideration, it is assumed that $\mathbf{H}$ is estimated perfectly and instantaneously at the receiver and this information is then fed back to the transmitter through an error-free delayless feedback path. This allows the transmitter to pre-filter the modulated symbols by the right singular matrix $\mathbf{V}$ to match the channel and, at the same time, the receiver filters the received signal by the left singular matrix $\mathbf{U}$ before demodulation and decoding. Through these filtering operations, the channel is naturally decomposed into $m = \min(r, t)$ uncorrelated subchannels as illustrated in Fig. 2.5 [36].

The question of how the channel state information is estimated and fed back to the transmitter is not addressed in this thesis. An interested reader can refer to [36] for an algorithm to track $\mathbf{U}, \mathbf{D}$ and $\mathbf{V}$ and the issue of feedback is addressed in [49] and references therein. In addition, [14, 50, 51] have also studied how accurate channel estimation needs to be before the capacity starts degrading.

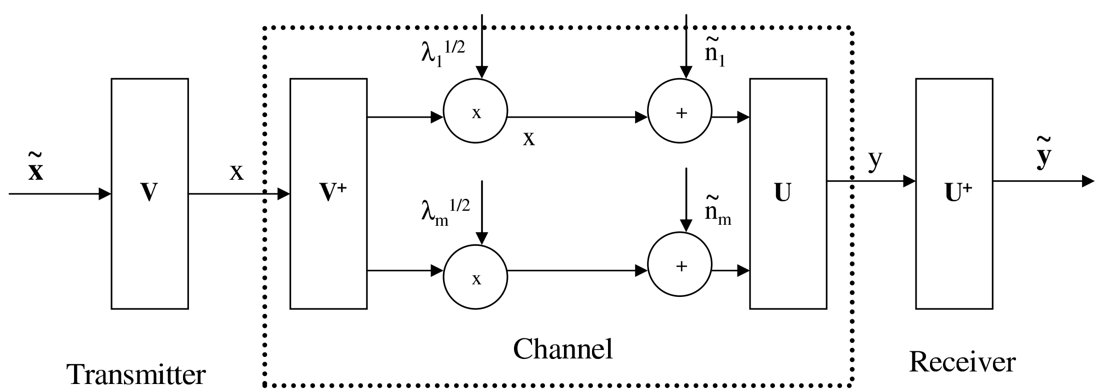

Figure 2.5: Multi-dimensional eigen-beamforming

Chapter 3

Channel Inversion and Truncated Channel Inversion

Achieving the Shannon capacity when the channel side information is available at both the transmitter and receiver requires the transmitter to adapt the power, data rate and coding scheme to the channel variation. This adds to the complexity of the transmitter and the receiver design. In this thesis, we present an adaptive transmission scheme for the MIMO channel that simplifies the transmitter and receiver design while exhibiting minimal capacity loss from the optimal.

3.1 Preliminaries

Channel Inversion (CI) is a simple adaptive technique in which the transmitter adjusts its power to invert the fading so as to maintain a constant SNR at the receiver [3]. This technique uses fixed-rate modulation and a fixed code design irrespective of the channel statistics, since the channel after CI appears as a time-invariant AWGN channel. As a result channel inversion with fixed rate is a relatively simple scheme to implement assuming good channel estimates are available at the transmitter and the receiver. The capacity for a single-antenna system using channel inversion was shown to be [3]

$$C = \log\left(1 + \frac{P}{\mathcal{E}\left[\frac{1}{\lambda_1}\right]}\right) . \tag{3.1}$$

However this scheme can exhibit a large capacity penalty relative to optimal adaptation in extreme fading environments like the Rayleigh fading environment since most of the average signal power is used to compensate for deep fades. However, when CI is combined with receive diversity, the capacity penalty decreases quickly with the number of diversity branches [29].

A better form of power control is truncated channel inversion (TCI) which only compensates for fading above a certain cutoff fade depth μ_1. A constant received SNR is maintained unless the channel fading falls below the cutoff value, in which case, a signal outage is declared and no signal is sent. The capacity for TCI in the single-antenna case was derived to be [3]:

$$C = \log\left(1 + \frac{P}{\mathcal{E}_{\mu_1}\left[\frac{1}{\lambda_1}\right]}\right) p\left(\lambda_1 \geq \mu_1\right) \tag{3.2}$$

where $\mathcal{E}_{\mu_1}\left[\frac{1}{\lambda_1}\right] = \int_{\mu_1}^{\infty} \frac{1}{\lambda_1} p(\lambda_1) d\lambda_1$ and $p(x)$ is the probability distribution function of x.

In this thesis, we investigate channel inversion and truncated channel inversion schemes in the context of MIMO systems. Ergodic capacity results for these schemes are derived assuming that perfect CSI available at the transmitter is used to invert the fade value in each of the subchannels obtained through multi-dimensional eigen-beamforming. Outage capacity, defined as the maximum rate below which arbitrarily reliable transmission is possible for a pre-specified percentage of channel realizations, is explored for CI and TCI and the results compared with the outage capacities of adaptive and nonadaptive transmission. The main advantage of CI and TCI is that it allows us to use a fixed constellation and hence we consider constellation-constrained capacities as well.

During the course of our work, we became aware of similar research that sought to apply channel inversion to multiple-antenna systems. In particular [37] investigates CI for MIMO systems under flat fading conditions. In addition, Scaglione *et al* examined channel inversion for MIMO systems under frequency-selective conditions [38] and Hochwald *et al* looked at applying channel inversion to the multiuser scenario [39]. But unlike these papers, we do not constrain the SNRs in each subchannel of our decomposed MIMO system to be equal, but instead for a fixed average transmitter power, we derive optimal SNR targets that maximize the overall capacity of the channel [52]. The removal of the equal SNR constraint enables our scheme to exhibit superior performance.

3.2 Ergodic Capacity

The main focus of this thesis as mentioned above is channel inversion (CI), a simpler suboptimal transmitter adaptation scheme where the transmitter uses the CSI to maintain a constant received SNR [14]. For the MIMO channel (2.5), channel inversion seeks to maintain a constant target SNR, say σ_i, in each of the m subchannels. As a consequence, at the receiver each subchannel becomes a time-invariant AWGN channel with SNRs $\sigma_1, \ldots, \sigma_m$. Although suboptimal, channel inversion is attractive because it enables the transmitter to employ a fixed constellation and to leverage the extensive literature on codes designed for the AWGN channel.

The power control policy employed in the i-th subchannel for channel inversion is

$$P_i = \frac{\sigma_i}{\lambda_i} \tag{3.3}$$

where σ_i is the target received SNR selected for the i-th subchannel. These received SNRs are chosen to satisfy an overall power constraint:

$$P = \sum_{i=1}^{m} \sigma_i \mathcal{E}\left[1/\lambda_i\right] \ . \tag{3.4}$$

For MIMO channels with $m > 1$, there is the additional question of how best to select the received SNRs $\sigma_1, \ldots, \sigma_m$ subject to the constraint (3.4). (For $m = 1$, σ_1 is uniquely determined by this constraint.) Information theory offers an immediate answer to this question: Note that the ergodic capacity of the channel (2.5) with channel inversion (3.7) is just the sum of the capacities of parallel AWGN channels with SNRs $\sigma_1, \sigma_2, \ldots, \sigma_m$ [3]

$$C_{CI} = \sum_{i=1}^{m} \log\left(1 + \sigma_i\right) \ . \tag{3.5}$$

It is convenient to write this in terms of the average transmitted power $\bar{P}_i = \sigma_i \mathcal{E}[1/\lambda_i]$:

$$C_{CI} = \sum_{i=1}^{m} \log\left(1 + \frac{\bar{P}_i}{\mathcal{E}[1/\lambda_i]}\right) \tag{3.6}$$

in which case the constraint becomes $\sum_i \bar{P}_i = P$. From this, it is now clear that C_{CI} is maximized by a modified form of water-filling distribution

$$\bar{P}_i = \left(\frac{1}{\lambda_o} - \mathcal{E}\left[\frac{1}{\lambda_i}\right]\right)^+ \ . \tag{3.7}$$

In related work on channel inversion for MIMO systems [37, 38, 39], the authors constrain the SNRs in all subchannels to be equal. This implies that $\sigma_1 = \sigma_2 = \ldots = \sigma_m$ and the capacity for a single channel realization was shown to be

$$C = \sum_{i=1}^{m} \log\left(1 + \frac{P}{\sum_{i=1}^{m} \frac{1}{\lambda_i}}\right) = m \log\left(1 + \frac{P}{\sum_{i=1}^{m} \frac{1}{\lambda_i}}\right) \ . \tag{3.8}$$

Averaging this over fading statistics, we obtain the ergodic capacity and it is given by:

$$C = \mathcal{E}\left[m \log\left(1 + \frac{P}{\sum_{i=1}^{m} \frac{1}{\lambda_i}}\right)\right] \tag{3.9}$$

where $\mathcal{E}$ here denotes expectation with respect to the random gains $\lambda_1, \ldots, \lambda_m$ of the subchannels. This scheme although it provides a constant SNR across all subchannels does not provide a time-invariant SNR. When we extend their result to fit our premise of providing an AWGN channel at all times to the receiver, the ergodic capacity of this scheme referred to as channel inversion with equal SNR is then given by:

$$C = m \log\left(1 + \frac{P}{\sum_{i=1}^{m} \mathcal{E}[1/\lambda_i]}\right) \ . \tag{3.10}$$

In [53], it is shown that capacity varies with the number of subchannels used and at certain SNRs the optimum number of subchannels that maximize capacity is less than m. If we denote $\hat{k}$ as the optimum number of subchannels, the ergodic capacity for the channel inversion with equal SNR is:

$$C(\hat{k}) = \hat{k} \log\left(1 + \frac{P}{\sum_{i=1}^{\hat{k}} \mathcal{E}[1/\lambda_i]}\right) \tag{3.11}$$

and $\hat{k}$ is optimized as

$$\hat{k} = \arg \max_{k=1,\ldots,m} C(k) \ , \tag{3.12}$$

Note that the optimal power allocation in our scheme — channel inversion with optimal SNR (3.6) is a water-filling distribution (3.7) and this automatically takes care of switching off degraded channels. Moreover, it is natural to see that since we derive optimal SNRs for each subchannel that maximize capacity, our capacity (3.6) will always be greater than or equal to (3.11).

It is well known that the capacity with channel inversion in Rayleigh fading for single-antenna systems is zero [14]. Similarly for MIMO systems, whenever $t = r$, channel inversion suffers a capacity penalty from the optimal adaptive capacity, although usually the capacity is not zero. This is because whenever we have a system with equal number of transmit and receive antennas, the time average of the inverse eigenvalues of the m-th subchannel obtained by decomposition (2.5), i.e, $\mathcal{E}[1/\lambda_m]$ is infinite [57] and this prevents us from transmitting any data on that subchannel. However, since the quantities $\mathcal{E}[1/\lambda_i]$ are finite for $t \neq r$ [57], channel inversion is expected to work well for asymmetric MIMO channels.

As noted in [14], in cases where channel inversion performs poorly, a modified power control scheme, called truncated channel inversion (TCI), often performs significantly better. In TCI for MIMO channels, channel inversion is used in the i-th subchannel only when λ_i exceeds a fixed cutoff, say $\mu_i \geq 0$; otherwise the transmitter sends nothing $(x_i = 0)$. Thus, the power control policy is

$$P_i = \begin{cases} \frac{\sigma_i}{\lambda_i}, & \lambda_i \geq \mu_i \\ 0, & \lambda_i < \mu_i \end{cases} \tag{3.13}$$

and the power constraint is

$$P = \mathcal{E}\left[\sum_{i=1}^{m} P_i\right] = \sum_{i=1}^{m} \sigma_i p(\lambda_i \geq \mu_i)\mathcal{E}[1/\lambda_i | \, \lambda_i \geq \mu_i] \, . \tag{3.14}$$

Once again, $\sigma_1, \ldots, \sigma_m$ and $\mu_1, \ldots, \mu_m$ need to be chosen so as to maximize the ergodic capacity of the resulting MIMO system:

$$C_{TCI} = \sum_{i=1}^{m} p(\lambda_i \geq \mu_i) \log\left(1 + \sigma_i\right) \tag{3.15}$$

Proceeding as above, this capacity can be written as as

$$C_{TCI} = \sum_{i=1}^{m} p(\lambda_i \geq \mu_i) \log\left(1 + \frac{\bar{P}_i}{\mathcal{E}[1/\lambda_i |\, \lambda_i \geq \mu_i]}\right) \tag{3.16}$$

where $\bar{P}_i = \mathcal{E}[P_i |\, \lambda_i \geq \mu_i] = \sigma_i \mathcal{E}[1/\lambda_i |\, \lambda_i \geq \mu_i]$ is the power allocated to the i-th subchannel when it is "on", and the corresponding power constraint is $\sum_{i=1}^{m} p(\lambda_i \geq \mu_i)\bar{P}_i = P$. In general, optimizing this quantity with respect to $\mu_1, \ldots, \mu_m$ is quite difficult and best performed numerically. For fixed $\mu_1, \ldots, \mu_m$, however, it is easy to verify that the optimal power distribution is once again a water-filling distribution:

$$\bar{P}_i = \left(\frac{1}{\lambda_o} - \mathcal{E}\left[\left.\frac{1}{\lambda_i}\right|\, \lambda_i \geq \mu_i\right]\right)^+ . \tag{3.17}$$

3.3 Outage Capacity

So far in this chapter, we have looked at ergodic or mean capacity. Outage capacity is another performance measure that can be used to characterize an information system. Outage capacity is roughly understood as the maximum rate below which arbitrarily reliable transmission is possible for a pre-specified percentage of channel realizations [54]. The outage probability q at rate R and power constraint P is given by

$$q = Pr\left\{C\left(\lambda_1, \ldots, \lambda_m\right) < R\right\} , \tag{3.18}$$

where $C(\lambda_1, \ldots, \lambda_m)$ is the channel capacity of a random MIMO channel characterized by gains $\lambda_1, \ldots, \lambda_m$. For any $q \in (0, 1)$, the resulting outage capacity, denoted by $C(q)$, is

$$C(q) = \sup\{R \geq 0 : Pr\{C(\lambda_1, \ldots, \lambda_m) < R\} \leq q\} \tag{3.19}$$

Our channel inversion scheme has a constant non-zero capacity (3.5) every channel realization except when $t = r = 1$. This is often referred to as a zero outage capacity scheme [55] since there is 0% probability that there is no transmission. The same is not true however for truncated channel inversion. In TCI, transmission occurs in subchannel i only if the instantaneous fade value λ_i is greater than the cutoff value μ_i of the subchannel. The outage capacity for this scheme is defined by (3.19), where

$$C(\lambda_1, \ldots, \lambda_m) = \sum_{i=1}^{m} 1(\lambda_i \geq \mu_i) \log(1 + \sigma_i) \tag{3.20}$$

and $1(x)$ is the indicator function whose value is 1 when $x > 0$ and 0 otherwise. The σ_is and μ_is are derived to maximize ergodic capacity as described in Sec. 3.1. It is important to note that the σ_is and μ_is that optimize the ergodic capacity may not necessarily optimize outage capacity.

Following along similar lines, outage capacities for adaptive and nonadaptive transmission can be derived. The instantaneous channel realization capacity for adaptive transmission is derived as

$$C(\lambda_1, \ldots, \lambda_m) = \sum_{i=1}^{m} \log_2(1 + P_i \lambda_i) \tag{3.21}$$

where the P_is are chosen according to the water-filling distribution (2.12) to maximize ergodic capacity.

For nonadaptive transmission, the capacity is

$$C(\lambda_1, \ldots, \lambda_m) = \sum_{i=1}^{m} \log_2 \left(1 + \frac{P}{t}\lambda_i\right) \ . \tag{3.22}$$

3.4 Constellation-Constrained Capacity

As noted before, one of the attractive features of channel inversion is that the transmitter may employ a fixed constellation and error-control code designed for the AWGN channel. Note that each finite complex constellation entails some loss of capacity relative to a Gaussian input and, since different subchannels have different SNRs, each subchannel may require a different constellation. Capacities obtained when fixed constellations are transmitted on each subchannel are considered next.

Let $a^k, 0 \leq k < M$, denote the complex signal points in a unit-energy M-ary complex signal constellation $\mathcal{C}$. For a single-antenna AWGN channel with received SNR σ, the constellation-constrained capacity under the assumption of equiprobable occurrence of input signals is given by [46, 56]

$$\begin{aligned} CC_{\mathcal{M}}(\sigma) = \log_2(M) - & \\ & \frac{1}{M}\sum_{k=0}^{M-1} \mathcal{E}\left\{\log_2\left(\sum_{j=0}^{M-1} \exp\left(A_k\right)\right)\right\} \end{aligned} \tag{3.23}$$

where $A_k = -(|\sqrt{\sigma}a^k + n - \sqrt{\sigma}a^j|^2 - |n|^2)$ and $\mathcal{E}$ denotes the expectation with respect to the noise variable $n \sim \mathcal{CN}(0,1)$.

Consider now the MIMO channel (2.5) with channel inversion power control (3.7). Since channel inversion converts each subchannel to an AWGN channel, the ergodic constellation-constrained capacity is

$$CC_{CI} = \sum_{i=1}^{m} CC_{\mathcal{M}_i}(\sigma_i) \tag{3.24}$$

where $\mathcal{M}_i$ and σ_i are the constellation and received SNR for the i-th subchannel, and the power constraint is (3.4). It is important to recognize that CC_{CI} is not necessarily optimized by choosing $\bar{P}_i = \sigma_i \mathcal{E}\left[1/\lambda_i\right]$ according to the water-filling distribution (3.7). Similarly, the ergodic constellation-constrained capacity for truncated channel inversion is given by

$$CC_{TCI} = \sum_{i=1}^{m} p(\lambda_i \geq \mu_i) CC_{\mathcal{M}_i}(\sigma_i) \ , \tag{3.25}$$

where $\sigma_1, \ldots, \sigma_m$ and $\mu_1, \ldots, \mu_m$ are subject to the power constraint (3.14). Again, this is not necessarily optimized by the water-filling distribution (3.17).

3.5 Numerical Results

Since optimal adaptation offers significant capacity gains over nonadaptive transmission only when $t > r$ [23], we focus our attention mainly on this case.

Fig. 3.1 plots the ergodic channel capacity of different transmission schemes (optimal adaptation, channel inversion with optimal SNR, channel inversion with equal

SNR and nonadaptive transmission) for the case of 4 transmit and 2 receive antennas as a function of the average transmit power to noise power ratio (average transmit SNR). We find that in comparison to optimal adaptation (2.11), channel inversion with optimal SNR (3.5) suffers a penalty of around 1 dB while channel inversion with equal SNR (3.10) incurs a penalty of approximately 2.5 dB at high SNRs. At low SNRs, CI with optimal SNR and CI with equal SNR are similar since it is optimal to allocate power across the first subchannel alone. Truncated channel inversion (3.15) yields a small increase in capacity relative to channel inversion with optimal SNR, but the gain diminishes with increasing transmit power. All of these schemes do improve considerably on the capacity of nonadaptive transmission (2.14).

Fig. 3.2 plots the same capacity curves for 8 transmit and 2 receive antennas. It is seen that with an increase in capacity, the penalty due to channel inversion with optimal SNR relative to adaptive capacity is now less than 0.5 dB. The gap between channel inversion with optimal SNR and channel inversion with equal SNR is also reduced. This is due to the fact that $\mathcal{E}\left[1/\lambda_i\right]$s of the subchannels become similar as the diversity increases. The capacity improvement provided by truncated channel inversion compared to total channel inversion is also relatively small and this little improvement comes at the expense of increased complexity since the transmitter has to switch 'on' and 'off' depending on the channel conditions. This suggests that as long as diversity is used, total channel inversion is a better alternative than truncated channel inversion especially since the receiver sees an AWGN channel all the time.

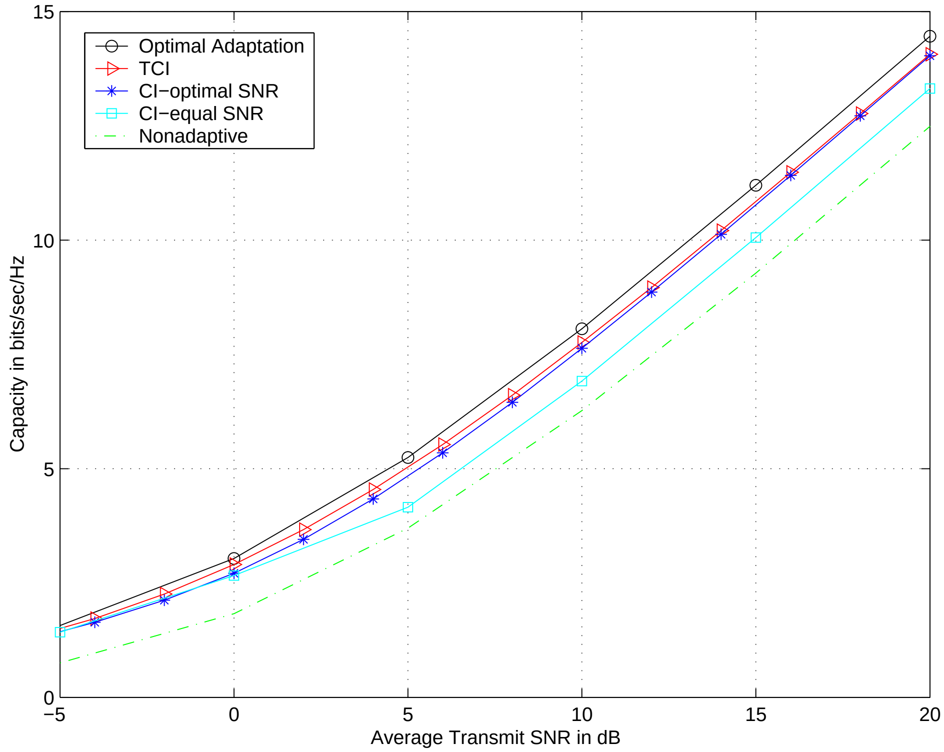

Figure 3.1: Ergodic capacities of different transmission schemes for a 4×2 MIMO system

The only scenario where truncated channel inversion can perform significantly better than channel inversion with optimal SNR is when $t = r$ as is illustrated in Fig. 3.3. We find that the inability to use the second subchannel due to an infinite $\mathcal{E}\left[1/\lambda_2\right]$ leads to a large capacity penalty for channel inversion as the SNR increases.

The complementary cumulative distribution function (CCDF) for the outage capacities of optimal adaptation, truncated channel inversion, channel inversion with optimal SNR and nonadaptive transmission are plotted in Fig. 3.4 and 3.5 for a 4×2 system with transmit SNRs 0 dB and 20 dB. It is important to note that various parameters in these transmission schemes have been optimized for ergodic capacity

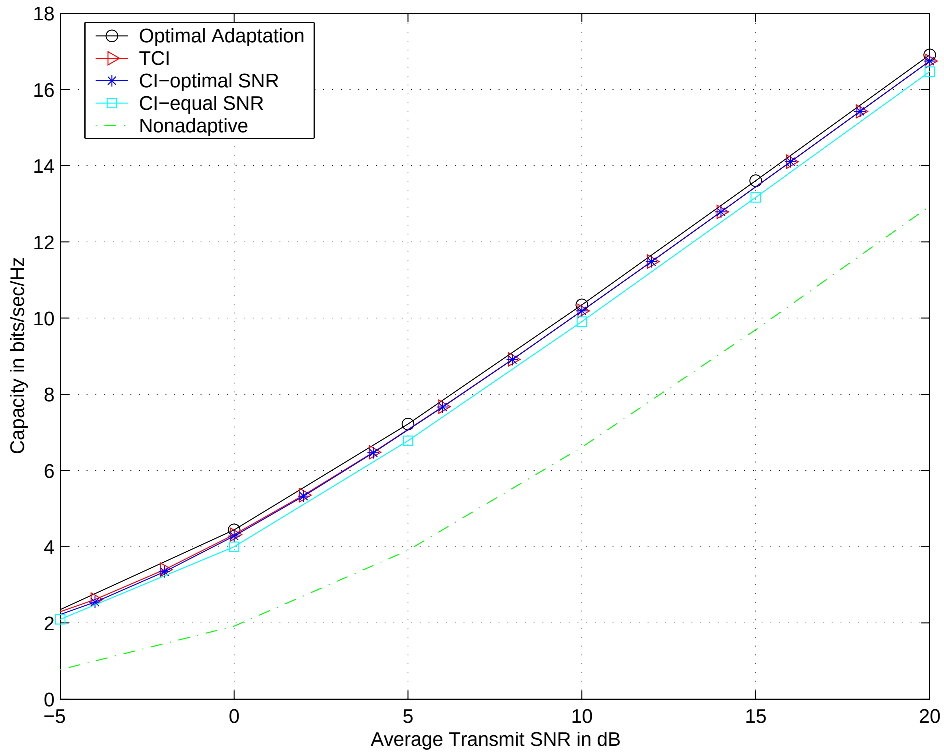

Figure 3.2: Ergodic capacities of different transmission schemes for a 8×2 MIMO system

and not for outage capacity and so the outage capacity curves can be suboptimal. As expected channel inversion does not suffer any outage (time when nothing is transmitted) and exhibits a constant capacity for all channel realizations. The CCDF of TCI is a step function on the y-axis. In Fig. 3.4, the CCDF of TCI has four steps corresponding to the fraction of time one or both subchannels are used or not used. The step corresponding to the proportion of time when only the second subchannel is used, is relatively small and hardly visible in the plot. As power (transmit SNR) increases, the probability of one or both subchannels being used increases and so the step corresponding to no transmission tends to reduce/vanish and the the outage

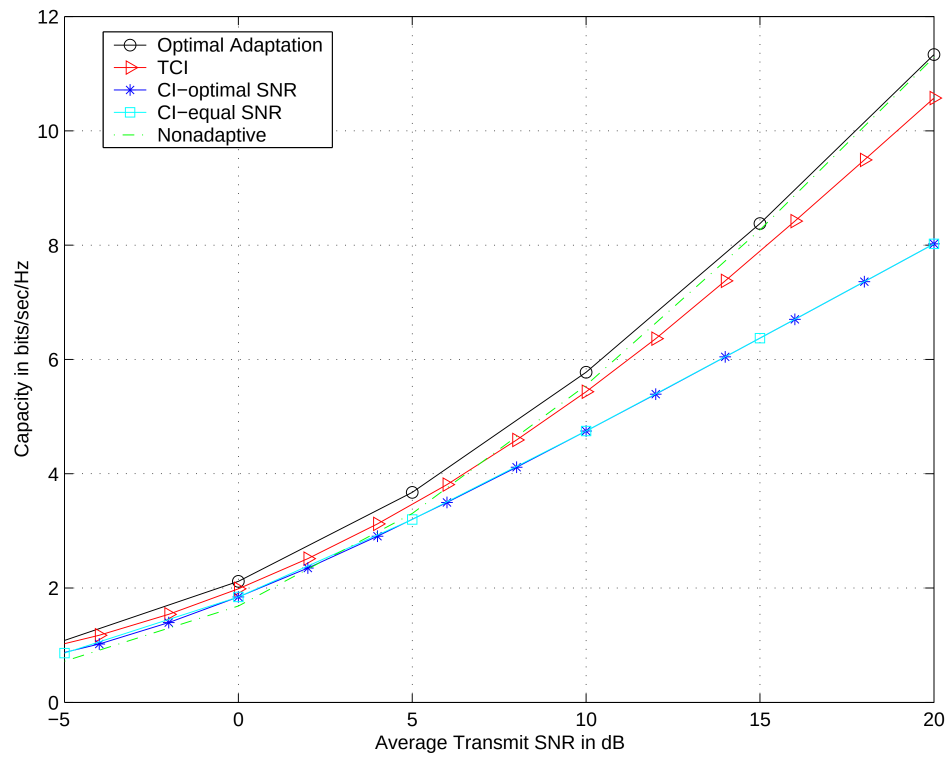

Figure 3.3: Ergodic capacities of different transmission schemes for a 2×2 MIMO system

capacity of TCI tends to mimic that of CI. We also find that CI and often TCI perform better at lower outage probabilities than optimal adaptive transmission. This is because adaptive transmission scheme waits for a few good channels to send the bulk of its data.

The same outage capacity curves are plotted for a 8×2 system with transmit SNRs 0 dB and 20 dB in Fig. 3.6 and 3.7. We observe the same trends as before as power increases. When we compare the capacity curves for 8×2 and 4×2 systems we find that increase in diversity also leads to both subchannels being used more often, i.e, the probability of either of the subchannels being in outage is reduced. This is

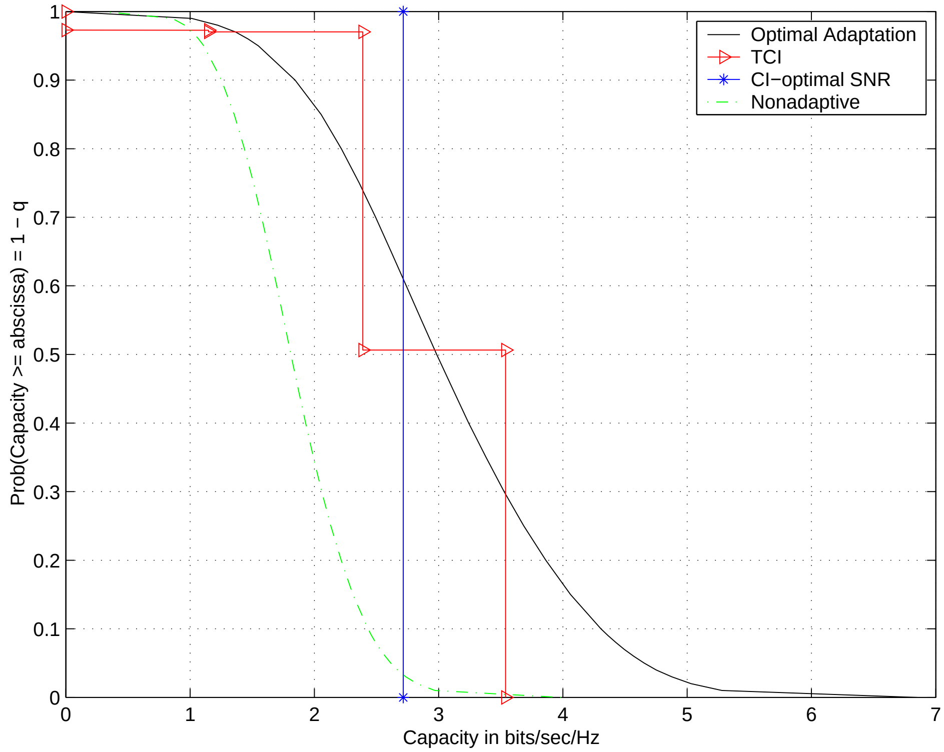

Figure 3.4: Outage capacities of different transmission schemes for a 4×2 MIMO system with transmit SNR $= 0$ dB

because the channel statistics improve with increasing diversity.

Figs. 3.8 and 3.9 show plots for the constellation-constrained capacities when channel inversion is used with fixed M-QAM constellations, where $M = 0, 2, 4, 8, \ldots$ constellations are transmitted in one or both of the subchannels of a 4×2 and 8×2 MIMO system. For example to obtain a spectral efficiency of 2, either 4-QAM can be transmitted in the best subchannel and nothing at all in the second ($M_1 = 4, M_2 = 0$) or 2-QAM can be transmitted ($M_1 = 2, M_2 = 2$) in the two subchannels. Since the plots get cluttered, only one of the combinations of M-QAM that gives a particular integer capacity has been plotted. For the case above, using just the first

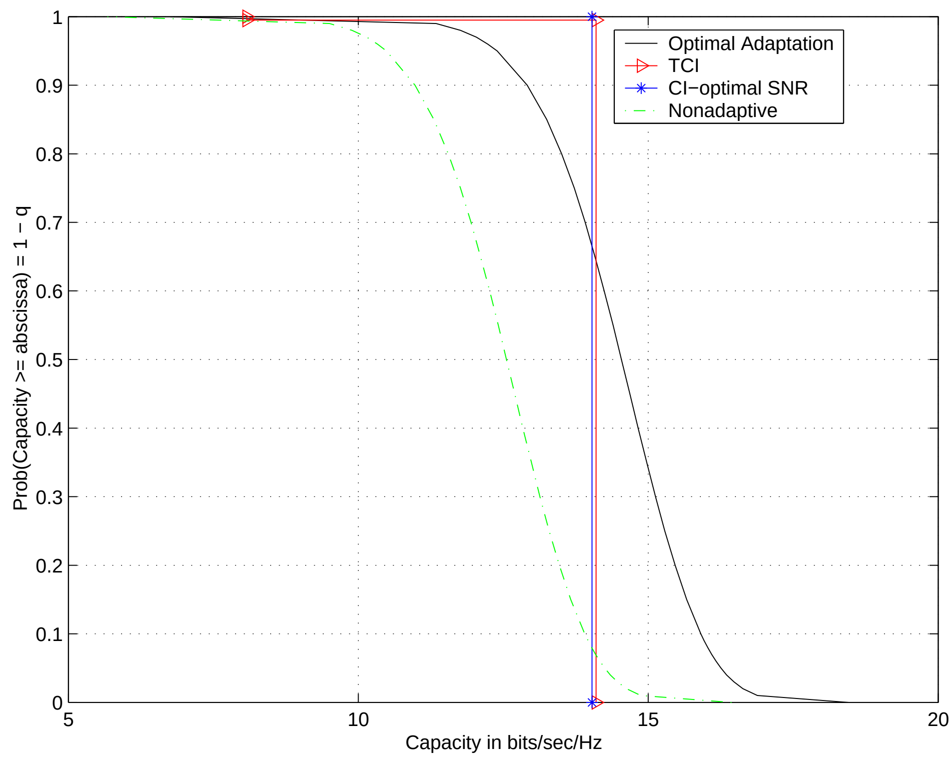

Figure 3.5: Outage capacities of different transmission schemes for a 4×2 MIMO system with transmit SNR = 20 dB

subchannel and transmitting 4-QAM gives the best results in terms of bits/sec/Hz in both figures for both channel inversion and truncated channel inversion. The constellation-constrained capacity curves for CI and TCI hug their respective capacity curves at low rates, but as the rate increases the constellation-constrained capacity curves saturates. TCI gives a benefit at low SNRs but as the SNR and diversity increases, the benefit is reduced. Moreover the benefit is more pronounced in cases where both subchannels are used.

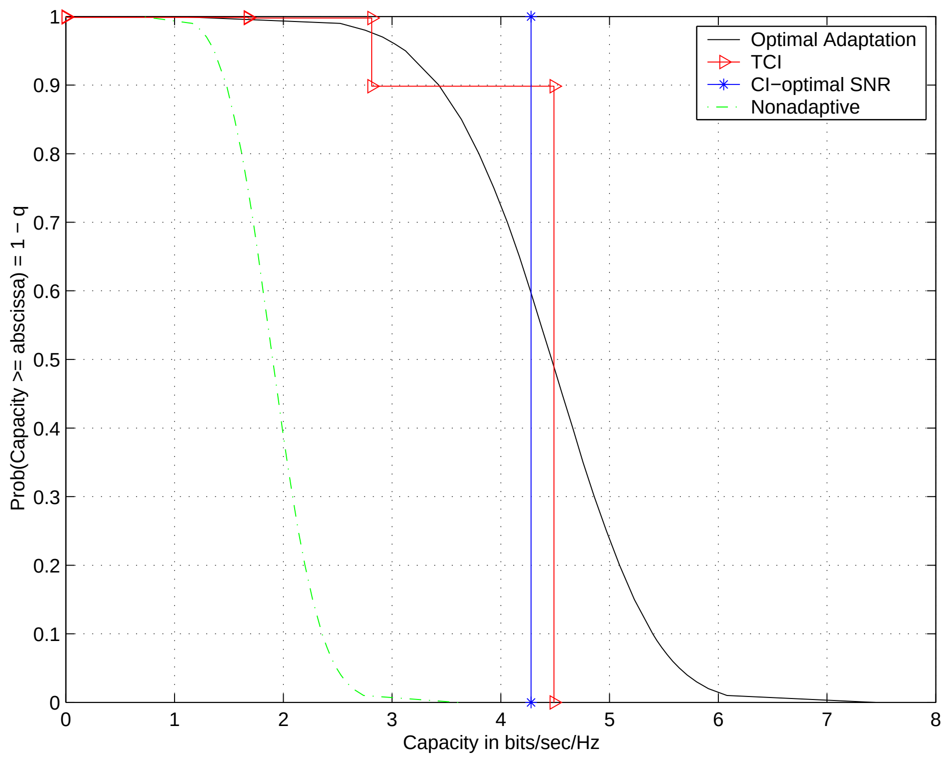

Figure 3.6: Outage capacities of different transmission schemes for a 8×2 MIMO system with transmit SNR $= 0$ dB

3.6 Conclusion

A simple adaptive transmission scheme that combines channel inversion with multi-dimensional beamforming was proposed in this chapter. In this scheme, the fade level in each of the subchannels obtained by decomposition of the original MIMO channel is inverted so as to maintain a constant SNR at the receiver. For any fixed average transmitter power, SNR targets for each beamformer that maximize the overall capacity of the channel were derived, and it was shown that these targets obey a weighted waterfilling distribution (3.5). Although these transmission schemes are

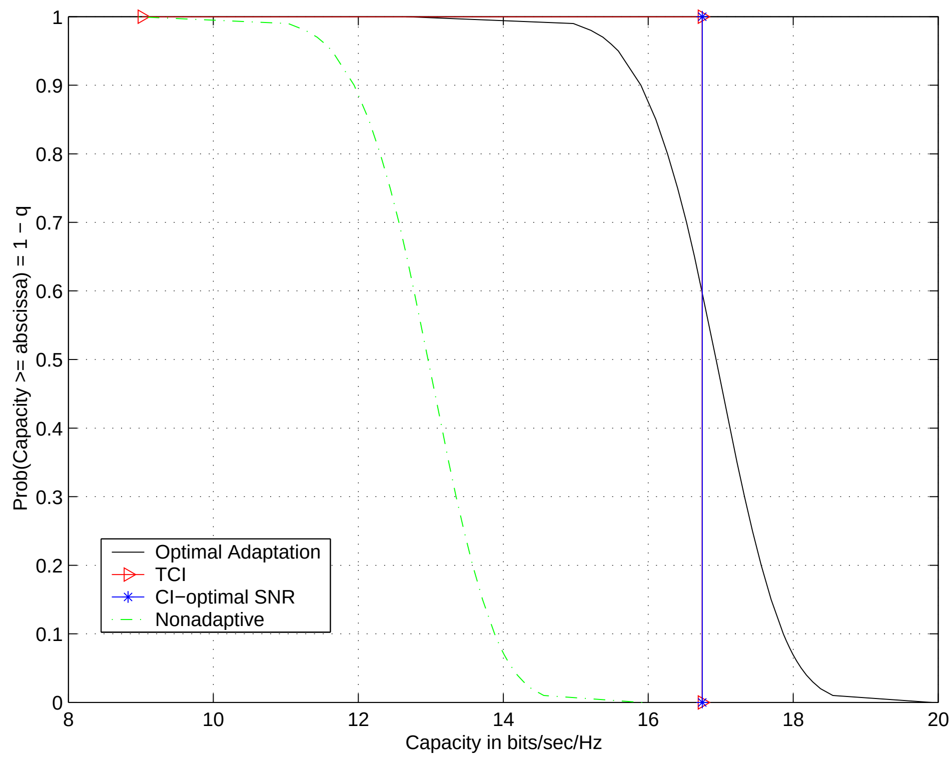

Figure 3.7: Outage capacities of different transmission schemes for a 8×2 MIMO system with transmit SNR $= 20$ dB

suboptimal, numerical results suggest that the capacity loss is often small, even for relatively few transmit and receive antennas, and vanishes as the number of antennas increases. For all but the smallest MIMO systems, the results suggest that most of the adaptive capacity of MIMO channels can be achieved by systems that combine eigen-beamformer channel inversion with fixed constellations and error-control codes designed for the AWGN channel.

Our scheme improves on the transmission scheme used in [37, 38, 39] since we do not constrain the SNRs across the subchannels to be equal. The improvement does however become negligible as the asymmetric diversity increases.

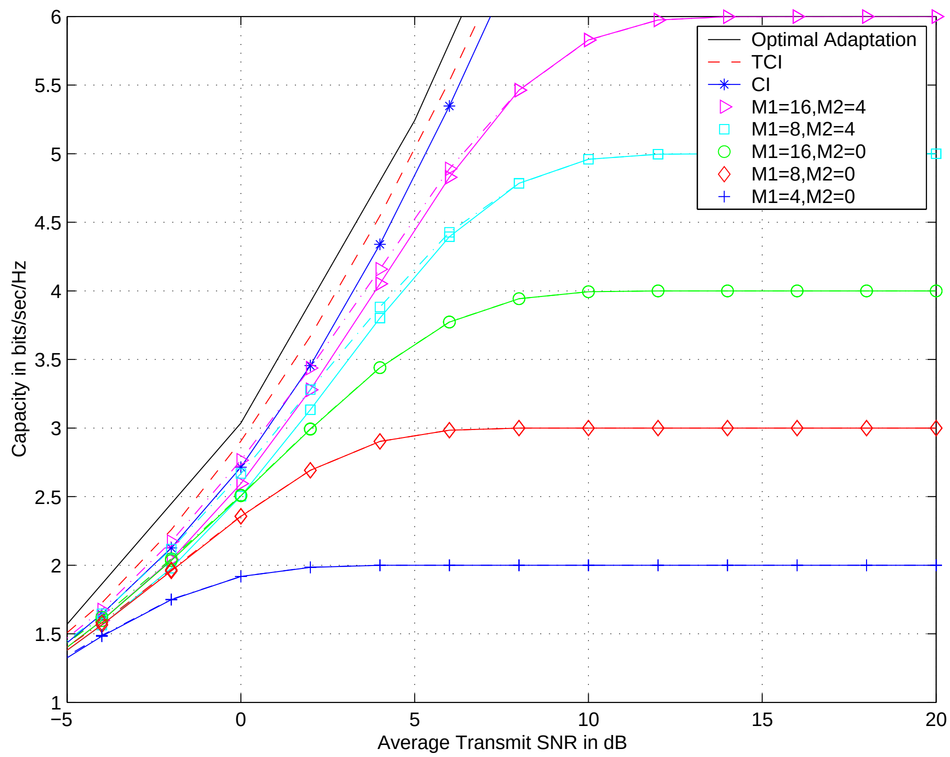

Figure 3.8: Constellation-constrained capacity for M-QAM used with CI (solid) and TCI (dashed) in a 4×2 system

Truncated channel inversion improves on channel inversion with optimal SNR, but the improvement in ergodic capacity is negligible as the average transmit power and/or diversity increases. Moreover this improvement comes at the expense of a probability of outage and increased receiver complexity. Channel inversion is preferable to truncated channel inversion since the receiver sees a constant AWGN channel and this naturally leads to a simple receiver design. Since there is no outage associated with the scheme and no rate adaptation, buffering of data is not required. It is beneficial to use truncated channel inversion only when the number of transmit and receive antennas are equal. However TCI can usually achieve a larger outage capacity

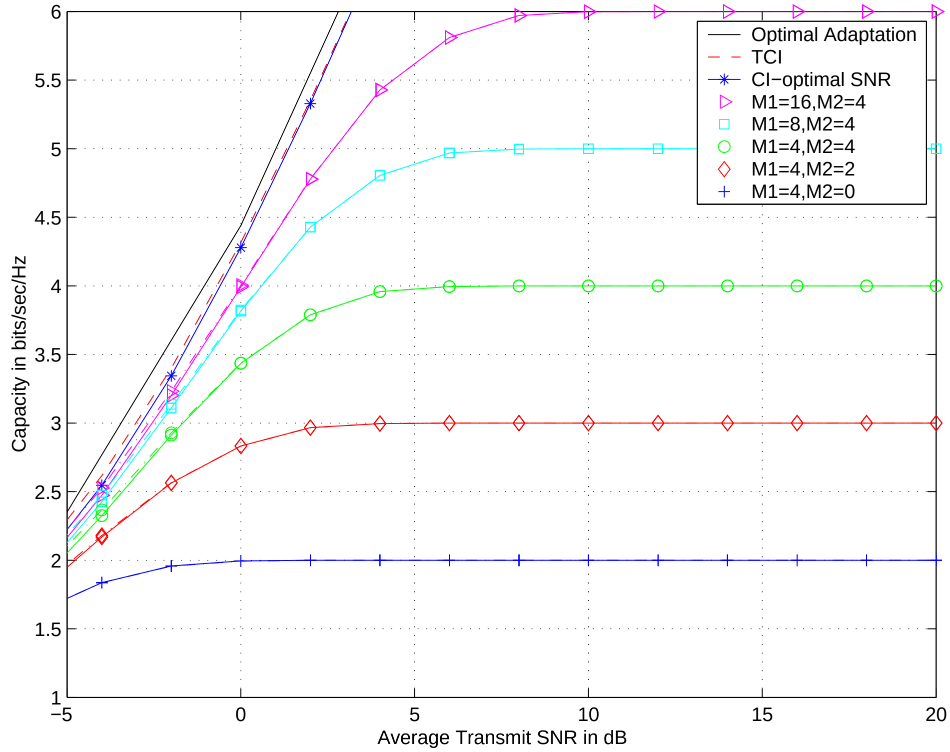

Figure 3.9: Constellation-constrained capacity for M-QAM used with CI (solid) and TCI (dashed) in an 8×2 system

than CI in all $t \times r$ systems.

Constellation-constrained capacities when a fixed constellation is used in conjunction with channel inversion in each of the subchannels obtained from the MIMO channel is also examined and it is seen that the results follow the trend of AWGN channels.

Chapter 4

Turbo Trellis-Coded Modulation

4.1 Preliminaries

Capacity can be defined as the maximum rate at which data can be transmitted reliably over the channel. In his pioneering work [58], Shannon proved that there exists random codes with large block lengths that achieve performances close to capacity. However, a method to construct such codes was not provided. So it is important to look at practical adaptive modulation methods and compare their spectral efficiency relative to the theoretical maximum as described in Chapter 3.

A variable-rate variable-power M-ary quadrature amplitude modulation (M-QAM) scheme was shown in [14] to exhibit a 20 dB power gain over nonadaptive modulation for a single-antenna system in a Rayleigh flat fading environment. This scheme did not consider coding and this resulted in an 11 dB gap from optimal adaptive Shannon capacity for a BER of 10^{-6}. Trellis codes superimposed on adaptive modulation improved on the uncoded case but was still 6 dB away from capacity [15]. Adaptive turbo-coded modulation was considered in [18] whereby the transmit rate was adapted by adapting the channel encoder itself and this scheme came within 3 dB of capacity. Adaptive modulation schemes for multiple-antenna systems based on channel statistics were derived in [34, 35], and in [23] the design of adaptive space-time codes that exploit partial transmitter channel state information was investigated.

In the previous chapter, we presented a scheme which can exploit the extensive literature on coding for AWGN channels. Channel inversion in conjunction with multi-dimensional beamforming brings us close to the optimal adaptive capacity of the channel and allows the receiver to see an AWGN channel. Turbo codes introduced in 1993 [40] can achieve near-capacity results at low SNRs in AWGN channels. However these binary codes are not suitable for bandwidth limited communications. Several attempts were made to extend turbo codes for higher order modulation; see [41, 42, 43, 44, 45] and references therein. In this chapter, we look at applying turbo trellis-coded modulation (TTCM) introduced by Robertson *et al* [43] to the channel inversion scheme described in Chapter 3.

4.2 Turbo Trellis-Coded Modulation

Turbo trellis-coded modulation is a bandwidth-efficient channel coding scheme in which the structure of binary turbo codes [40] is combined with Ungerboeck's trellis-coded modulation (TCM) scheme [59]. This combination of turbo codes with TCM component codes leads to a simple encoder structure allowing iterative decoding similar to the binary turbo decoder. Subsections 4.2.1 and 4.2.2 describe the generic encoder and decoder structure for the TTCM scheme.

4.2.1 TTCM Encoder

The general structure of the TTCM encoder is shown in Fig. 4.1 [63], where two Ungerboeck TCM codes of rate $\frac{m}{m+1}$ are concatenated in a parallel manner via a symbol interleaver. Each encoder is then followed by a signal mapper. The encoder operates on N groups of m information bits, where N is the interleaver size. The $m+1$ output bits of each encoder are mapped to the appropriate QAM constellation based on the Ungerboeck set partitioning method [59]. The symbol interleaver is restricted to permuting the information bits in a symbol-wise way, i.e, it is not allowed to change the ordering of m information bits arriving at the interleaver at any given time. The interleaver is also constrained to map even positions to even positions and odd ones to odd ones.

Before transmission over the channel, the output of the second encoder is dein-

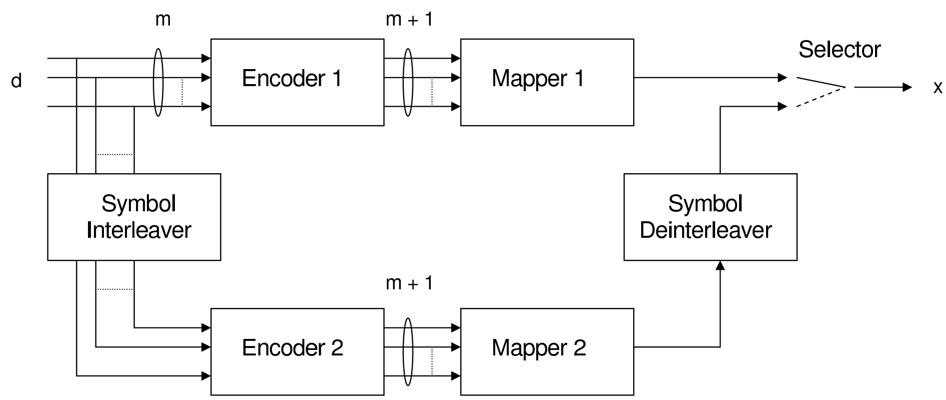

Figure 4.1: Turbo Trellis-Coded Modulation Encoder

terleaved. This is done so that the m information bits which determine the parity bit of both the component encoders at a given time are identical. Since the m information bits are contained in the modulated signals coming from both encoders, a selector is used to transmit symbols alternately from the two mappers. This ensures that the information bits are not transmitted twice. In this way, a throughput of m bits/sec/Hz is achieved.

For the component trellis code, all of the m input bits may not be encoded. In practice, the uncoded bits would not need to pass through the interleaver but can be directly used to select the final signal point from a subset of points after the selector [43].

4.2.2 TTCM Decoder

Performing maximum-likelihood decoding for turbo codes is a tedious task. Fortunately iterative decoding algorithms in which component decoders exchange soft information about the reliability of each decoded bit can give near-optimal performance. The component decoders can use the soft-output Viterbi algorithm (SOVA) [60] to generate the soft outputs. This algorithm minimizes the sequence error probability, but this does not necessarily translate into minimum symbol error probability. So if the performance criteria is minimum symbol error probability, the Maximum A-Posteriori (MAP) decoding algorithm derived in [61] is optimal.

The iterative decoder for TTCM is similar to the one used to decode binary turbo codes [40, 62] except that the symbol probability is passed from one decoder to the other rather than the bit probability. However with the MAP algorithm, there is a tendency for the soft outputs to become either too large or too small, causing computational overflows. So, in this thesis, we use a modified MAP algorithm called the symbol-by-symbol log-MAP algorithm [43, 63] in which logarithm of probabilities is computed and passed to the next stage.

Each group of m information bits d_k is represented by an integer i in the range $(0, 1, \ldots, 2^m - 1)$ and is associated with the transition from time $k-1$ to k. The state of the encoder at each step k is denoted by S_k. In the remainder of this subsection, M', M and M'' denotes the state of the encoder at time $k-1, k$ and $k+1$ respectively i.e. $S_{k-1} = M'$, $S_k = M$ and $S_{k+1} = M''$, where $M', M, M'' \in (0, 1, \ldots, 2^{\nu})$ and ν is the memory of the encoder . The output of the encoder at time k is mapped to the symbol x_k. The receiver observes N noisy symbols where each symbol is associated with each step in the trellis, i.e., from step $k-1$ to step k the receiver observes y_k and the total received sequence is given by $\mathbf{y} = \mathbf{y_1^N} = (y_1, y_2, \ldots, y_N)$.

The goal of the decoder is to calculate the log-likelihood ratio (LLR) of each group of m information bits. The symbol i with the largest LLR is chosen as the hard decision output. The soft output $L(d_k = i)$ is given by

$$L(d_k = i) = \log \frac{Pr(d_k = i|\mathbf{y}_1^N)}{Pr(d_k = 0|\mathbf{y}_1^N)} \tag{4.1}$$

In order to evaluate this, some variables are defined as follows:

$$\alpha_{k-1}(M') = \log Pr\left(S_{k-1} = M', \mathbf{y_1^{k-1}}\right) \ , \tag{4.2}$$

$$\beta_k(M) = \log Pr\left(\mathbf{y_{k+1}^N}|S_k = M\right) \ , \tag{4.3}$$

$$\begin{aligned} \gamma_k^i(M', M) &= \log Pr\left(d_k = i, S_k = M, y_k|S_{k-1} = M'\right) \\ &= \log Pr(d_k = i) + \log Pr\left(y_k|x_k\right) + \log Pr(x_k|M', M) \end{aligned} \tag{4.4}$$

The first term in (4.4) represents the a-priori probability of $d_k = i$ and $Pr(d_k = i|M', M)$ is either zero or one depending on whether the encoder input $i \in (0, 1, \ldots, 2^m - 1)$ is associated with the transition from state $S_{k-1} = M'$ to $S_k = M$ or not.

Using these variables, (4.1) can be written as

$$L(d_k = i) = \log\left[\frac{\sum_M \sum_{M'} e^{\alpha_{k-1}(M') + \gamma_k^i(M', M) + \beta_k(M)}}{\sum_M \sum_{M'} e^{\alpha_{k-1}(M') + \gamma_k^0(M', M) + \beta_k(M)}}\right] \tag{4.5}$$

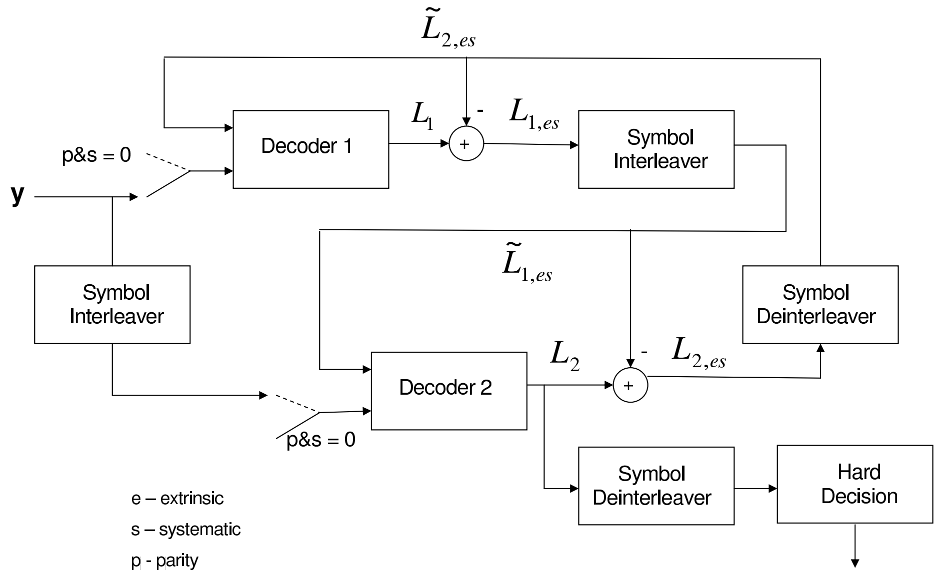

Figure 4.2: Turbo Trellis-Coded Modulation Decoder

The forward recursive variable $\alpha_k(M)$ can be computed recursively as follows:

$$\alpha_k(M) = \log \sum_{M'} \sum_{i} e^{\alpha_{k-1}(M') + \gamma_k^i(M',M)} \tag{4.6}$$

with the initial conditions $\alpha_0(0) = 0$ and $\alpha_0(S_0) = -\infty, S_0 \neq 0$.

The backward recursive variable $\beta_k(M)$ can be computed as

$$\beta_k(M) = \log \sum_{M''} \sum_{i} e^{\beta_{k+1}(M'') + \gamma_{k+1}^i(M,M'')} \tag{4.7}$$

with the initial condition $\beta_N(S_N) = 0$.

The iterative process of the symbol-by-symbol MAP algorithm is similar to that of binary turbo decoders except that there is a difference in the nature of information passed between the two component decoders [43]. For the binary turbo decoder, the soft output can be split into three terms — the a-priori information generated by the other decoder, the systematic information generated by the m information bits and the extrinsic information generated by all other inputs. Only the extrinsic information is usually exchanged between the two component decoders. However in the case of TTCM, the systematic component cannot be separated from the extrinsic information since both the parity and the systematic components are mapped to a single symbol. Thus both the components will be passed to the next decoder as shown in Fig. 4.2 [43, 63]. The joint extrinsic and systematic information of the first log-MAP decoder denoted by $L_{1,es}$ can be obtained as

$$L_{1,es}(d_k = i) = L_1(d_k = i) - \log Pr(d_k = i) \tag{4.8}$$

The interleaved version of the $L_{1,es}(d_k = i)$ denoted by $\tilde{L}_{1,es}(d_k = i)$ is used as the a-priori probability by the second decoder in the next step. The extrinsic and systematic information of the second decoder is given by

$$L_{2,es}(d_k = i) = L_2(d_k = i) - \tilde{L}_{1,es}(d_k = i) \tag{4.9}$$

In the next iteration, the a-priori probability in (4.8) is replaced by the deinterleaved extrinsic and systematic information from the second decoder represented by $\tilde{L}_{2,es}(d_k = i)$.

In the MAP algorithm, it is important that the component decoders avoid using the same systematic information twice in every iterative decoding step. In TTCM, this is taken care of by the fact that each decoder alternately receives the noisy output of its own encoder and that of the other encoder due to the puncturing by the selector. For example, during odd time intervals, the first decoder generates soft outputs based on the symbols generated by its own encoder. However during even time intervals, the decoder receives the symbols generated by the other encoder. The decoder in this case ignores the symbol and generates a soft output based on the a-priori component obtained from the other decoder.

It is important to note that the second decoder always has a-priori information available. This is true also of the first decoder except in the very first decoding stage. The algorithm relies on the use of a-priori input during the time the decoder encounters a punctured symbol. The transmitted symbol for the punctured transmission is determined by the information group d_k and by the unknown parity bit $b^0 \in 0, 1$ produced by the other encoder. By applying Bayes' rule, the a-priori information can be derived as

$$Pr(d_k = i) = const \sum_{j \in (0,1)} p(y_k | d_k = i, b_k^0 = j) \tag{4.10}$$

where the value of the constant can be obtained by normalizing over all i [43]. If the symbol for which a-priori information is being considered is not a punctured transmission, the a-priori information is

$$Pr(d_k = i) = \frac{1}{2^m} \tag{4.11}$$

The iterative process continues and with each iteration the symbol error probability reduces. However the improvement in performance for each additional iteration decreases as the number of iterations increases. At the end of a fixed number of iterations, the soft output from the second decoder $L_2(d_k = i)$ is deinterleaved and a hard decision is made by choosing the symbol i with the largest LLR.

4.3 TTCM with Channel Inversion

Turbo trellis-coded modulation is used in each of the subchannels obtained after multi-dimensional eigen-beamforming along with channel inversion. The different TTCM encoders mapped to different M-QAM constellations used in this thesis are given in Table. 4.1. The his in Table. 4.1 represent different octal generator polynomials used by each component TCM encoder to generate codes. Note that all encoders have constraint length 4. To obtain a particular spectral efficiency, different combinations of TTCM encoders from Table. 4.1 can be used in all or a subset of the subchannels. We constrain the BER in each subchannel to be the same and find the total power required to transmit at that particular spectral efficiency with a BER of 10^{-4}. A frame length of 1024 was considered and the decoder was made to carry out eight iterations.

Fig. 4.3 and Fig. 4.4 shows the spectral efficiencies of TTCM when used with channel inversion and multidimensional beamforming in a 4×2 and 8×2 system. To avoid clutter, only the combination of TTCM encoders that give the best performance is plotted for a particular spectral efficiency. For example, in the 4×2 case, using just

Table 4.1: TTCM encoders

M-QAM	State	$h0$	$h1$	$h2$	$h3$
4	8	13	04		
8	8	11	02	04	
16	8	11	02	04	10
32	8	11	02	04	10

the first subchannel and transmitting the encoder in the first row of Table. 4.1 mapped to 8-QAM gives the best results for a spectral efficiency of two. It can be observed that this TTCM scheme performs within 3 dB of the channel inversion capacity and it is less than 4 dB away from the optimal adaptive capacity.

4.4 Conclusion

Turbo trellis-coded modulation is a bandwidth-efficient scheme that gives good results in AWGN channels. Hence it was used along with channel inversion on each of the subchannels obtained by multi-dimensional eigen-beamforming. For a frame size of 1024 and 8 decoding iterations using log-MAP algorithm, it was found that this scheme performs within 4 dB of the Shannon adaptive capacity of the MIMO channel. The gap between the spectral efficiency and capacity is expected to reduce if a larger frame size and/or better encoders and interleavers are used [62, 64]. Using some of the newer codes that perform extremely well in AWGN channels like asymmetric turbo codes [45] and low-density parity-check codes [65] is expected to give results that are

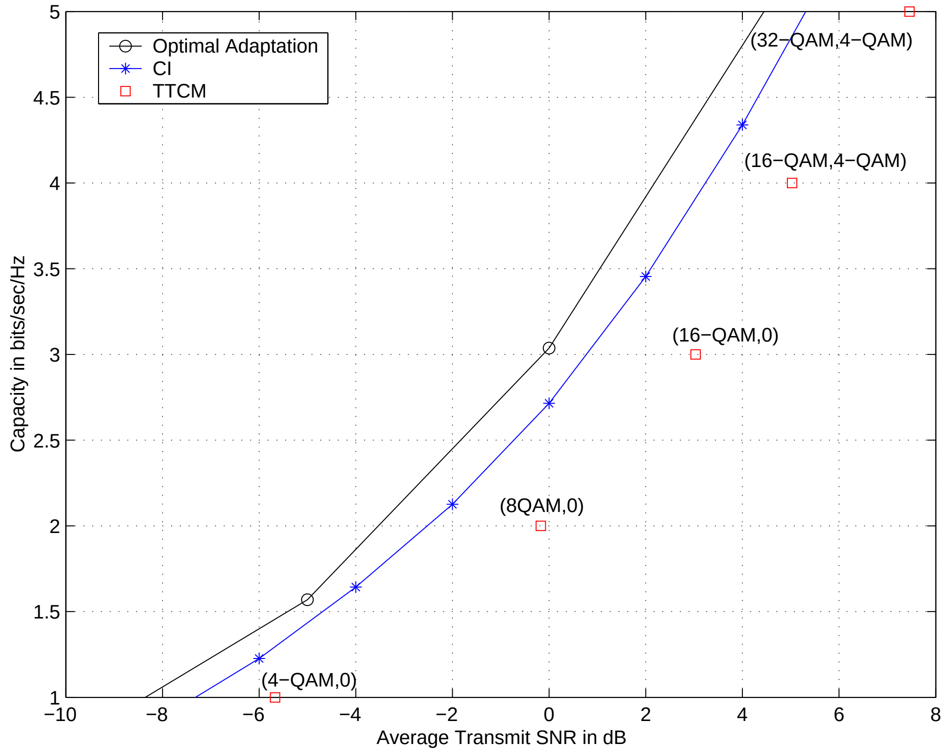

Figure 4.3: Spectral efficiency of TTCM with CI for a 4×2 MIMO system

closer to the optimal adaptation capacity.

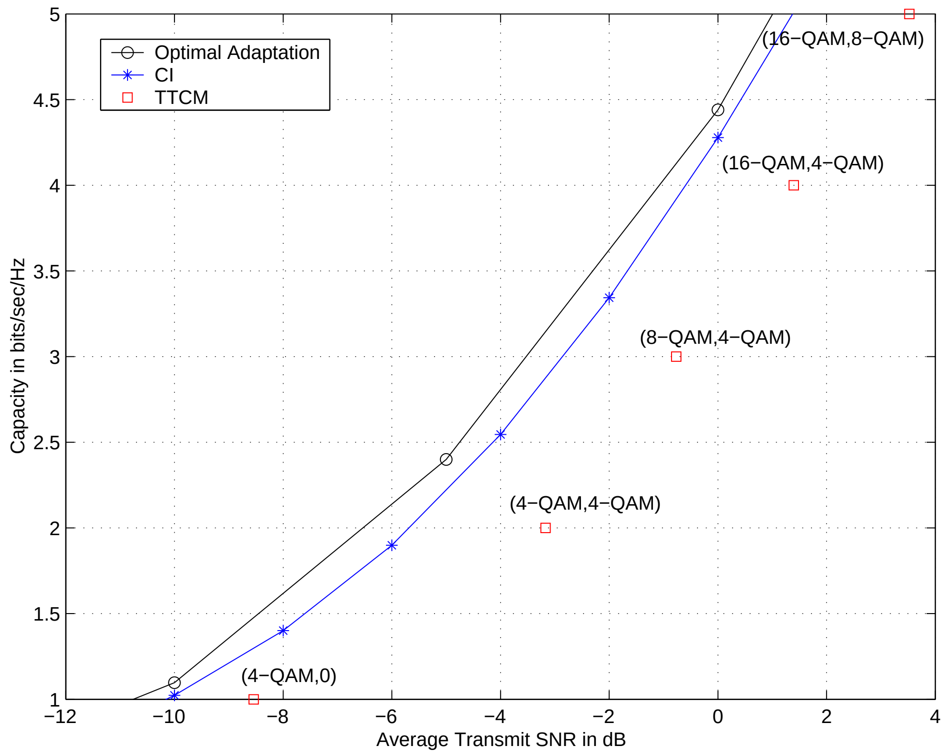

Figure 4.4: Spectral efficiency of TTCM with CI for a 8×2 MIMO system

Chapter 5

Conclusions

Adaptive modulation can often lead to significant increases in capacity for Rayleigh fading MIMO channels. This scheme requires both the transmitter and the receiver to know the instantaneous channel state information and the transmitter uses this knowledge to adapt various signal parameters like transmit power, rate and coding to increase spectral efficiency. However this can be quite complex to implement and so in this thesis we introduce a scheme in which channel inversion is used in conjunction with multi-dimensional eigen-beamforming (decomposition of MIMO channels into parallel uncorrelated subchannels through prefiltering using singular unitary matrices). Channel inversion reduces complexity since only the power is adapted at the transmitter and the receiver always sees an AWGN channel. For a fixed transmitter power, SNR targets for each beamformer that maximize the overall capacity are derived and it is shown that they obey a water-filling distribution. Though suboptimal, this scheme suffers a capacity penalty of only about 1 dB in the 4×2 case and this gap reduces as the number of transmitters increases.

Truncated channel inversion for MIMO systems is also investigated and it is found that the capacity gain relative to channel inversion is minimal as the diversity and power increases. Moreover when we explored outage capacities, we found that truncated channel inversion suffers an outage probability whenever the instantaneous fade value falls below a certain cutoff value. This complicates design since the transmitter has to buffer data during periods in which no transmission takes place and the receiver sees an 'on' and 'off' AWGN channel. Given that truncated channel inversion usually leads to only minor performance improvement over channel inversion, we conclude that most of the optimal adaptation capacity of a MIMO channel can be attained by systems that combine eigen-beamformer channel inversion with fixed constellations and error-control codes designed for the AWGN channel. It is advantageous to use truncated channel inversion only when we have a MIMO system with equal number of transmit and receive antennas since in this scenario, channel inversion loses the ability to use one of the subchannels due to the statistics of the fade values.

The main advantage of both channel inversion and truncated channel inversion is that it allows us to transmit fixed constellations. So we investigate constellation-constrained capacities when channel inversion and truncated channel inversion schemes are used with fixed M-QAM constellations in each of the subchannels. A practical coding scheme — turbo trellis-coded modulation is implemented and it is found that it comes within 4 dB of capacity. Other coding schemes can perhaps give better results but have not been explored in this thesis.

The success of the scheme given in this thesis depends on how well the channel is tracked at the receiver and how well that information is fed back to the transmitter. In [36], a channel estimation algorithm is given and in the future, the performance of our channel inversion scheme can be evaluated with the practical channel tracking algorithm. Throughout this thesis, we assume that we have perfect instantaneous knowledge of the channel at both transmitter and receiver. Considering imperfect estimates as well as quantized feedback might also lead to interesting results.

Bibliography

[1] J-Z. Sun, J. Sauvola and D. Howie, "Features in future:4G visions from a technical perspective," *IEEE Global Telecommunications Conference,* vol. 6, pp.3533-3537, Nov. 2001.

[2] B. Sklar, "Raleigh fading channels in mobile digital communication systems .I. Characterization," *IEEE Comm. Magazine,* vol. 35, no. 7, pp. 90-100, Jul. 1997.

[3] A. J. Goldsmith and P. P. Varaiya, "Capacity of fading channels with channel side information," *IEEE Trans. Inform. Theory,* vol. 43, no. 6, pp. 1986-1997, Nov. 1997.

[4] J. F. Hayes "Adaptive feedback communications," *IEEE Trans. Commun. Technol.,* vol.COM-16, pp. 29-34, Feb. 1998.

[5] B. Narendran, J. Sienicki, S. Yajnik and P. Agrawal, "Evaluation of an adaptive power and error control algorithm for wireless systems," *Proc. ICC'97,* vol. 1, pp. 349-355, 1997.

[6] J. K. Cavers, "Variable-rate transmission for Rayleigh fading channels, " *IEEE Trans. Commun.,* vol. COM-22, pp. 1331-1337, Sept. 1974

[7] W. T. Webb and R. Steele, "Variable rate QAM for mobile radio," *IEEE Trans. Commun.,* vol 43, pp. 2223-2230, Jul. 1995.

[8] Y. Kamio, S. Sampei, H. Sasaoka and N. Morinaga, "Performance of modulation-level-controlled adaptive-modulation under limited transmission delay time for land mobile communications," *Proc. IEEE Veh. Technol. Conf,* pp. 221-225, Jul. 1995.

[9] J. M. Torrance and L. Hanzo, "Optimisation of switching levels for adaptive modulation in slow rayleigh fading," *Electron. Lett,* vol. 32, no. 13, pp. 1167-1169, Jun. 1996.

[10] J. M. Torrance and L. Hanzo, "Adaptive modulation in a slow Rayleigh fading channel," *IEEE International Symposium on Personal, Indoor and Mobile Radio Communications,* vol. 2, pp. 497-501, Oct. 1996.

[11] B. Vucetic, "An adaptive coding scheme for time-varying channels," *IEEE Trans. Commun.,* vol. 39, pp. 653-663, May 1991.

[12] V. K. N. Lau and M. D. Macleod, "Variable rate adaptive trellis-coded QAM for high bandwidth efficiency application in Rayleigh fading channels," *Proc. IEEE Veh. Technol. Conf.,* vol. 1, pp. 348-352, 1998.

[13] B. Myhre, V. Markhus and G. E. Oien, "LDPC-coded adaptive modulation on slowly varying Nakagami-fading channels," *Proc. European Wireless'02,* pp. 822-828, 2002.

[14] A. J. Goldsmith and S.-G. Chua, "Variable-rate variable-power MQAM for fading channels," *IEEE Trans. on Commun.,* vol. 45, no. 10, pp. 1218-1230, Oct. 1997.

[15] A. J. Goldsmith and S.-G. Chua, "Adaptive coded modulation for fading channels," *IEEE Trans. on Commun.,* vol. 46, no. 5, pp. 595-602, May. 1998.

[16] S. M. Alamouti and S. Kallel, "Adaptive trellis-coded multiple-phased-shift keying for Rayleigh fading channels, " *IEEE Trans. Commun.,* vol 42, pp. 2305-2314, Jun. 1994.

[17] T. Ue, S. Sampei and N. Morinaga, "Symbol rate and modulation level controlled adaptive modulation/TDMA/TDD for personal communication systems," *IEICE Trans. Commun.,* vol. E78-B, pp. 1117-1124, Aug. 1995.

[18] S. Vishwanath and A. Goldsmith, "Adaptive turbo-coded modulation for flat-fading channels," *IEEE Trans. on Commun.,* vol. 51, no. 6, pp. 964-972, Jun. 2003.

[19] A. Duel-Hallen, S. Hu, H. Hallen, "Long-range prediction of fading signals," *IEEE Sig. Processing,* vol. 17, no. 3, pp. 62-75, May. 2000.

[20] G. E. Oien, H. Holm and K. J. Hole, "Channel prediction for adaptive coded modulation in rayleigh fading," *Proc. European Signal Processing Conference,* Sept. 2002.

[21] D. L. Goeckel, "Adaptive coding for time-varying channels using outdated fading estimates," *IEEE Trans. on Commun.,* vol. 47, no. 6, pp. 844-855, Jun. 1999.

[22] S. Catreux, V. Erceg, D. Gesbert, R. W. Heath Jr., “Adaptive modulation and MIMO coding for broadband wireless data networks,” *IEEE Communications Magazine,* pp. 108-115, Jun. 2002.

[23] H. El Gamal and M. Bourles, “On the design of adaptive space-time codes,” *IEEE Trans. on Commun.,* vol. 52, no. 20, pp. 1670-1674, Dec. 2004.

[24] E. Telatar, “Capacity of multi-antenna gaussian channels,” *AT&T Bell Labs Internal Tech. Memo,* Jun. 1995.

[25] T. K. Yo, “Maximal ratio transmission,” *IEEE Trans. on Commun.,* vol. 47, pp. 1458-1469, Oct. 1999.

[26] M. Raitola, A. Hottinen and R. Wichman, “Transmission diversity in wideband CDMA,” em Proc. IEEE VTC’99,, vol. 2, pp. 1545-1549, May 1999.

[27] D. Rajan and S. D. Gray, “Transmit diversity schemes for CDMA-2000,” *Proc. IEEE Wireless Commun. and Network Conference,* vol. 2, pp. 669-673, Sept. 1999.

[28] K. Rohani, M.Harrison and K. Kuchi, “A comparison of base station transmit diversity methods for third generation cellular standard,” *Proc. IEEE VTC’99* vol. 1, pp. 351-355, May 1999.

[29] M.-S. Alouini and A. J. Goldsmith, “Capacity of Rayleigh fading channels under different adaptive rransmission and diversity combining techniques,” *IEEE Trans. on Vehicular Technology.,* vol. 48, no. 4, pp. 1165-1181, Jul. 1999.

[30] A. Narula, M. J. Lopez, M. D. Trott and G. W. Wornell, “Efficient use of side information in multiple-antenna data transmission over fading channels,” *IEEE J. Select Areas Commun.,* vol. 16, pp. 1423-1436, Oct. 1998.

[31] S. A. Jafar and A. Goldsmith, “On optimality of beamforming for multiple antenna systems with imperfect feedback,” *Proc. IEEE Int. Symp. Information Theory,* pp. 321, Jun. 2001.

[32] E. Visotsky and U. Madhow, “Space-time transmit precoding with imperfect feedback,” *IEEE Trans. Inform. Theory,* vol. 47, pp. 2632-2639, Sept. 2001.

[33] G. Jongren, M. Skoglund and B. Ottersen, “Combining beamforming and orthogonal space-time block coding,” *IEEE Trans. Inform. Theory,* vol. 48, pp. 611-627, Mar. 2002.

[34] S. Zhou and G. B. Giannakis, “Adaptive modulation for multiantenna transmissions with channel mean feedback,” *IEEE Trans. on Wireless Communications,* vol. 3, pp. 1626-1636, Sept. 2004.

[35] S. Zhou and G. B. Giannakis, "Optimal transmitter eigen-beamforming and space-time block coding based on channel correlations," *IEEE Trans. on Information Theory*, vol. 49, no. 7, pp. 1832-1840, Jul. 2003.

[36] A. Poon, D. Tse and R. Brodersen, "An adaptive multiantenna transceiver for slowly flat fading channels," *IEEE Trans. on Commun.,* vol. 51, no. 11, pp. 1820-1827, Nov. 2003.

[37] V. Jungnickel, T. Haustein, E. Jorswieck and C. von Helmolt, "On linear preprocessing in multi-antenna Systems," *IEEE Global Telecommunications Conference,* vol. 1, pp. 17-21, Nov. 2002.

[38] A. Scaglione, P. Stoica, S. Barbarossa, G. B. Giannakis and H. Sampath, "Optimal designs for space-time linear precoders and decoders," *IEEE Trans. on Signal Processing,* vol. 50, pp. 1051-1064, May. 2002.

[39] B. Hochwald and S. Vishwanath, "Space-time multiple access: linear growth in sum rate," *Proc. 40th Allerton Conference on Communications, Control and Computing,* Oct. 2002.

[40] C. Berrou, A. Glavieux and P. Thitimajshima, "Near Shannon-limit error-correcting coding and decoding: Turbo-codes," *Proc. ICC'93* pp. 1064-1070, May. 1993.

[41] S. Le Goff, A. Glavieux and C. Berrou, "Turbo-codes and high spectral efficiency modulation," *Proc. ICC'94* pp. 645-649, May. 1994.

[42] S. Benedetto, D. Divsalar, G. Montorsi and F. Pollara, "Parallel-concatenated trellis-coded modulation," *Proc. ICC'96* pp. 974-978, May. 1996.

[43] P. Robertson and T. Worz, "Bandwidth-efficient turbo trellis-coded modulation using punctured component codes," *IEEE Journal on Sel. Areas in Comm.,* vol. 16, no. 2, pp. 206-218, Feb. 1998.

[44] C. Fragouli and R. D. Wesel, "Turbo-encoder design for symbol-interleaved parallel-concatenated trellis-coded modulation," *IEEE Trans. on Comm.,* vol. 49, no. 3, pp. 425-435, Mar. 2001.

[45] D. J. Costello Jr., A. Banerjee, T. E. Fuja and P. C. Massey, "Some reflections on the design of bandwidth-efficient turbo codes," *Proc. of the 4th International ITG Conference on Source and Channel Coding,* pp. 357-363, Jan. 2002.

[46] G. Ungerboeck, "Channel coding with multi-level/phase signals," *IEEE Trans. Inform. Theory,* vol. IT-28, pp. 55-67, Jan. 1982.

[47] T. S. Rappaport, *Wireless Communications: Principles and Practice,* Prentice Hall, 1996.

[48] T. M. Cover and J. A. Thomas, *Elements of information theory,* Wiley-Interscience Publication, 1991.

[49] D. J. Love, R. W. Heath,Jr., W. Santipach and M. L. Honig, "What is the value of limited feedback for MIMO Channels?," *IEEE Commun. Magazine,* vol. 42, no. 10, pp. 54-59, Oct. 2004.

[50] S. Zhou and G. B. Giannakis, "How accurate channel prediction needs to be for transmit-beamforming with adaptive modulation over rayleigh MIMO channels?," *IEEE Trans. on Wireless Commun.,* vol. 3, no. 4, pp. 1285-1294, Jul. 2004.

[51] X. Tang, M.-S. Alouini and A. J. Goldsmith, "Effect of channel estimation error on M-QAM BER performance in Rayleigh fading," *IEEE Trans. on Commun.,* vol. 47, no. 12, pp. 1856-1864, Dec. 1999.

[52] C. M. James and B. L. Hughes, "Adaptive transmission using channel inversion for multiple antenna systems," *38th Annual Conference on Information Sciences and Systems,* Mar. 2004.

[53] V. Jungnickel, T. Haustein, V. Pohl and C. van Helmolt, "Link adaptation in a multi-antenna system," *57th IEEE Semiannual Vehicular Technology Conference,* vol. 2, pp. 862-866, Apr. 2003.

[54] H. Zhang and T. Guess, "Asymptotical Analysis of the Outage Capacity of Rate-Tailored BLAST," *IEEE Global Commun. Conference,* vol. 22, no. 1, pp. 1797-1801, Dec. 2003.

[55] A. J. Goldsmith, *Wireless Communications,* Cambridge University Press. To appear 2004.

[56] D. J. Costello Jr., J. Hagenauer, H. Imai, S. B. Wicker, "Applications of error-control coding," *IEEE Trans. Inform. Theory,* vol. 44, no. 6, pp. 2531-2560, Oct. 1998.

[57] E. Jorswieck, G. Wunder, V. Jungnickel, T.Haustein, "Inverse eigenvalue statistics for rayleigh and rician MIMO channels ," *IEEE Seminar on MIMO: Communications Systems from Concept to Implementations (Ref. No. 2001/175),* pp. 3/1 -3/6, Dec. 2001.

[58] C. E. Shannon, "A mathematical theory of communications," *Bell System Technical Journal,* vol. 27, pp. 379-423, Jul. 1948.

[59] G. Ungerboeck, “Trellis-coded modulation with redundant signal sets Part II: State of the art,” *IEEE Communications Magazine,* vol. 25, no. 2, Feb. 1987.

[60] J. Hagenauer and P. Hoeher, “A Viterbi algorithm with soft decision outputs and its applications,” *Proc. of IEEE Globecom Conference,* vol. 3, pp. 1680-1686, Nov. 1989

[61] L. R. Bahl, J. Cocke, F. Jelink and J. Rajiv, “Optimal decoding of linear codes for minimizing symbol error rate,” *IEEE Trans. on Informatin Theory,* vol. IT-20, pp. 284-287, Mar. 1974

[62] L. Hanzo, T. H. Liew and B. L. Yeap, *Turbo coding, turbo equalisation and space-time coding for transmission over fading channels,* John Wiley and Sons, Aug. 2002.

[63] B. Vucetic and J.Yuan, *Turbo codes: Principles and applications*, 1st edition, Kluwer Academic Publishers, Jan. 2000.

[64] H. Ogiwara and M. Yano, "Improvement of turbo trellis-coded modulation system," *IEICE Trans. Fundamentals,* vol.E81-A, no. 10, pp. 2040-2046, Oct. 1998.

[65] C. Sae-Young, G. D. Forney. Jr, T. J. Richardson and R. Urbanke, “On the design of low-density parity-check codes within 0.0045 dB of the Shannon limit,” *IEEE Comm. Letters,* vol. 5, no. 2, pp. 58-60, Feb. 2001.